

Novel D-Xylose Derivatives Stimulate Muscle Glucose Uptake by Activating AMP-Activated Protein Kinase α

Arie Gruzman,[†] Ofer Shamni,[†] Moriya Ben Yakir,[†] Daphna Sandovski,[†] Anna Elgart,[‡] Evgenia Alpert,[†] Guy Cohen,[†] Amnon Hoffman,[‡] Yehoshua Katzhendler,[§] Erol Cerasi,^{||} and Shlomo Sasson^{*†}

Departments of Pharmacology, Medicinal Chemistry, and Pharmaceutics, School of Pharmacy, Faculty of Medicine, The Hebrew University, 91120 Jerusalem, Israel, and Endocrinology and Metabolism Service, Department of Internal Medicine, Hadassah-Hebrew University Medical Center, 91120 Jerusalem, Israel

Received July 15, 2008

Type 2 diabetes mellitus has reached epidemic proportions; therefore, the search for novel antihyperglycemic drugs is intense. We have discovered that D-xylose increases the rate of glucose transport in a non-insulin-dependent manner in rat and human myotubes *in vitro*. Due to the unfavorable pharmacokinetic properties of D-xylose we aimed at synthesizing active derivatives with improved parameters. Quantitative structure–activity relationship analysis identified critical hydroxyl groups in D-xylose. These data were used to synthesize various hydrophobic derivatives of D-xylose of which compound **19** was the most potent compound in stimulating the rate of hexose transport by increasing the abundance of glucose transporter-4 in the plasma membrane of myotubes. This effect resulted from the activation of AMP-activated protein kinase without recruiting the insulin transduction mechanism. These results show that lipophilic D-xylose derivatives may serve as prototype molecules for the development of novel antihyperglycemic drugs for the treatment of diabetes.

Introduction

The World Health Organization has defined type 2 diabetes a worldwide epidemic and predicted that the number of people diagnosed with the disease would reach over 380 million in 2025. A major pathogenic defect in the disease is insulin resistance, which is characterized by the impeded capacity of peripheral tissues to utilize glucose effectively in face of hyperinsulinemia.¹ Hyperglycemia contributes to this phenomenon by downregulating the rate of glucose transport and utilization in peripheral tissues, most notably in skeletal muscle,^{2,3} which is the main consumer of glucose. Modern antidiabetic drug therapy aims at a strict regulation of glucose homeostasis to prevent late complications of diabetes. However, monotherapy and combination therapy with oral agents often fail to achieve near-normoglycemia in diabetic patients, hence the frequent need for insulin treatment.⁴ Therefore, the search for novel antidiabetic drugs is intense. Recent work on the molecular mechanisms mediating insulin- and non-insulin-dependent augmentation of glucose transport in insulin-sensitive tissues has identified new potential targets for antidiabetic drugs.⁴ Among these, the enzyme 5'-AMP-activated protein kinase (AMPK)^a emerges as a unique target for drug development, since in its active form it induces glucose transporter-4

(GLUT4) translocation to the plasma membrane of insulin-sensitive cells and thus increases glucose influx in a non-insulin-dependent manner.⁵ In view of the reduced insulin secretory capacity and peripheral insulin resistance of type 2 diabetic patients, this mechanism is extremely attractive.

We have discovered, and extensively investigated, a new regulatory pathway of carbohydrate metabolism, the phenomenon of glucose-induced downregulation of glucose transport, which is operative in a variety of cell types, most notably myotubes and skeletal muscle.^{2,4,6,7} In a search for various carbohydrates that mimic this effect of glucose, we screened various pentoses and made a unique discovery: high levels of D-xylose upregulated the glucose transport system in myotubes. We used D-xylose as a prototype molecule for the synthesis of active derivatives with adequate pharmacodynamic and pharmacokinetic parameters. We now report the results of this effort and describe the cellular and molecular mechanisms of action of D-xylose and such active hydrophobic derivatives.

Results and Discussion

D-Xylose Augments the Rate of Hexose Transport in Myotubes in a Dose- and Time-Dependent Manner. In a search for carbohydrates that regulate glucose transport in skeletal muscles, we tested the pentoses D-xylose, D-arabinose, D-lyxose, and D-ribose in cultured L6 myotubes. The myotubes were preconditioned for 24 h at 23.0 mM D-glucose, then washed, and incubated for up to 10 h in medium containing the same D-glucose concentration and 20.0 mM pentose. The cultures were thoroughly washed with PBS at room temperature at the indicated times to remove all extracellular carbohydrates, and the rate of dGlc uptake was measured. Figure 1A shows that the rate of hexose transport increased markedly within 6 h of exposure to D-xylose and D-arabinose (1.77 ± 0.03 - and 1.38 ± 0.02 -fold, respectively, over the basal rate) and then gradually declined and approached the basal uptake level at 10 h. D-Lyxose and D-ribose had no significant effect on the hexose transport capacity of the myotubes, nor did 20.0 mM nonmetabolizable

* To whom correspondence should be addressed. Phone: +972-2-675-8798. Fax: +972-2-675-8741. E-mail: ShlomoSasson@huji.ac.il.

[†] Department of Pharmacology.

[‡] Department of Pharmaceutics.

[§] Department of Medicinal Chemistry.

^{||} Endocrinology and Metabolism Service.

^a Abbreviations: AICAR, 5-aminoimidazole-4-carboxamide-1- β -ribofuranosyl 5- β -monophosphate; Akt/PKB, protein kinase B; AMPK, AMP-activated protein kinase; α MEM, α -minimal essential medium; BSA, bovine serum albumin; dGlc, 2-deoxy-D-glucose; DMF, dimethylformamide; DMSO, dimethyl sulfoxide; DNP, 2,4-dinitrophenol; DTT, dithiothreitol; FCS, fetal calf serum; GLUT, glucose transporter; MeGlc, 3-O-methyl-D-glucose; NFDM, nonfat dry milk; OPD, *O*-phenylenediamine; PBS, phosphate-buffered saline; PEG, polyethylene glycol; PPTS, pyridinium *p*-toluenesulfonic acid; QSAR, quantitative structure–activity relationship; SDS, sodium dodecyl sulfate; TCA, trichloroacetic acid; THF, tetrahydrofuran.

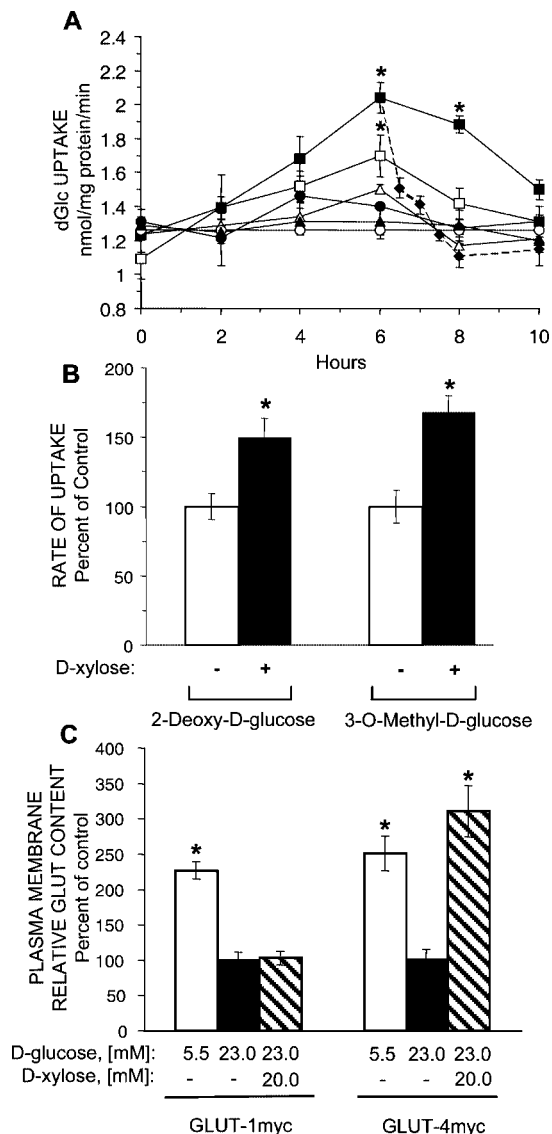


Figure 1. D-Xylose augments the rate of hexose transport in L6 myotubes in a dose- and time-dependent manner. (A) Time-course analysis. Myotube cultures were washed and received similar fresh medium supplemented with 20.0 mM D-xylose (■), D-arabinose (□), D-lyxose (●), or D-ribose (Δ). Control myotubes received fresh medium without (○) or with 20.0 mM L-glucose (▲). Myotubes incubated with 20.0 mM D-xylose for 6 h were washed and received fresh medium supplemented with 23.0 mM D-glucose (◆). The myotubes were then washed at the indicated times and taken for the standard [³H]dGlc uptake assay, as described in the Experimental Section. (B) Effect of D-xylose on the rate of MeGlc transport. L6 myotubes were pretreated as described above, washed and incubated in fresh medium supplemented with 20.0 mM D-xylose for 6 h, and taken for the [³H]MeGlc or [³H]dGlc uptake assays. The respective rates of uptake in myotubes that were not exposed to D-xylose (1.27 ± 0.08 nmol of dGlc (mg of protein)⁻¹ min⁻¹ and 1.02 ± 0.01 pmol of MeGlc (mg of protein)⁻¹ min⁻¹, respectively) were taken as the 100% values. (C) L6 myotubes expressing GLUT1myc and GLUT4myc were preconditioned and treated with 20.0 mM D-xylose for 6 h, as described above. At the end of incubation the cultures were taken for immunodetection of surface GLUT1myc or GLUT4myc. *, $p < 0.05$, in comparison with the respective control values following incubation at 23.0 mM glucose only.

glucose isomer L-glucose (Figure 1A). Importantly, the effects of D-xylose and D-arabinose were observed in the absence of insulin. A thorough washout of D-xylose from cultures at 6 h resulted in a rapid decline of the uptake rate, reaching the basal level within 90 min. Half-maximal and maximal stimulatory

effects of D-xylose were observed at 5.8 and 13.7 mM (Supporting Information Figure 1). Therefore, in further experiments we studied the maximal effect of D-xylose at 20 mM following 7 h of incubation.

To determine whether D-xylose increased the rate of hexose transport via glucose transporters, or also stimulated intracellular phosphorylation by hexokinase, we measured the rate of transport of the glucose analogue [³H]MeGlc, which, unlike dGlc, is not a substrate for hexokinase.⁸ Figure 1B shows that D-xylose induced comparable stimulations of dGlc and MeGlc accumulation in myotubes (1.51 ± 0.12 - and 1.69 ± 0.15 -fold above the respective control values), suggesting that D-xylose increased the plasma membrane content and/or activity of glucose transporters in L6 myotubes. To test this, we used L6 myotubes stably expressing GLUT1myc or GLUT4myc. The cell surface expression of these transporters was estimated by immunodetection of the myc epitope in an extracellular loop of the transporter.⁹ D-Xylose increased significantly the abundance of GLUT4myc, but not GLUT1myc, in the plasma membrane of L6 myotubes (Figure 1C). The figure also shows that the plasma membrane abundance of GLUT4myc and GLUT1myc in L6 myotubes exposed to 23.0 mM D-glucose for 24 h was reduced nearly by 50% compared to cultures maintained at 5.5 mM D-glucose. These findings confirm previous data on glucose-induced downregulation of glucose transporters in skeletal muscle^{2,7,10} and reconfirm the suitability of the myc-tagged L6 cell lines for investigating the muscle glucose transport system.

Although it has been shown that pentoses enter cells,¹¹ little is known about the pentose transport kinetics or pentose transporters in skeletal muscle. We therefore determined the kinetics of D-xylose transport in L6 myotubes. Figure 2A shows a saturable D-xylose influx into L6 myotubes, which reaches maximum within 30 s. Moreover, Figure 2B shows that D-xylose does not utilize glucose transporters to enter myotubes: when it was added directly to the [³H]dGlc uptake mixture, even at a concentration as high as 20 mM, this pentose failed to alter the rate of [³H]dGlc uptake. As expected, when unlabeled D-glucose and dGlc, which utilize glucose transporters to enter cells, were added to the uptake mixture, they reduced effectively and dose-dependently the accumulation of [³H]dGlc in the myotubes (Figure 2B). These data suggest the presence of a highly specific pentose transport system in skeletal muscles. Such a specific transporter of D-xylose explains well the ability of the pentose to exert significant biological effects in the presence of high concentrations of D-glucose.

D-Xylose was not added alone to myotube cultures in glucose-free medium because this condition mimics the effect of glucose starvation. Although D-xylose enters the cells, its intracellular metabolism is different from that of D-glucose and is unable to sustain the energy balance required for normal cell function. The findings the D-xylose and D-glucose utilize independent transport systems (Figure 2B) and that D-xylose augments the rate of hexose transport in myotubes already exposed to high D-glucose concentration (Figure 1A and 1B) indicate an important regulatory role of this pentose on the hexose transport system in hyperglycemic-like conditions.

Thus, we show for the first time that D-xylose is a potent stimulator of glucose uptake in myotubes by increasing the plasma membrane abundance of GLUT4 in a non-insulin-dependent manner. It is, however, evident that despite these remarkable qualities, D-xylose presents unfavorable pharmacokinetic and pharmacodynamic characteristics which excludes its consideration as a potential drug for the treatment of

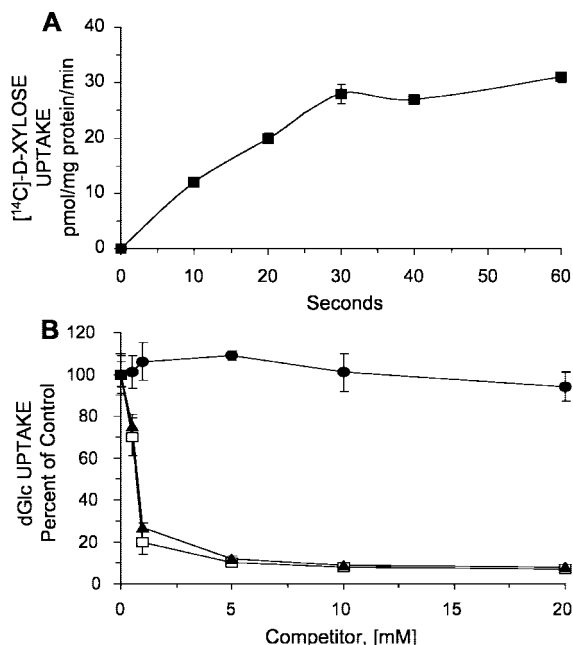


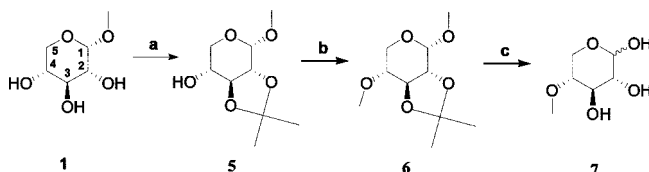
Figure 2. D-xylose uptake in L6 myotubes. The myotubes were preconditioned at 2.0 mM glucose for 24 h to increase the rate of hexose transport to the maximal level. (A) The cultures were washed at the indicated times and taken for the [¹⁴C]xylose uptake assay, as described in the Experimental Section. (B) Competition assay: similar myotube cultures were washed and taken for the [³H]dGlc uptake assay. However, the standard uptake mixture was supplemented with the indicated concentrations of nonradioactive D-glucose (□), dGlc (▲), or D-xylose (●). The basal rate of dGlc uptake in the standard uptake mixture (1.47 ± 0.09 nmol (mg of protein)⁻¹ min⁻¹) was taken as 100%.

hyperglycemia: its rate of influx is low, its effective extracellular concentration is very high (> 10 mM), its biological half-life is very short (30–60 min¹²), and its hexose transport-augmenting effect declines shortly after being washed out. Therefore, we used D-xylose as a prototype molecule for synthesis of long-acting and more potent derivatives.

QSAR of D-Xylose. A structure–activity relationship analysis of D-xylose was imperative to plan the synthesis of potent derivatives. Methyl ether derivatives of xenobiotics are intracellularly stable and not easily cleaved. Therefore, a selective methylation of each hydroxyl group in the D-xylose molecule was performed, and the capacity of the methylated derivatives to modulate the hexose transport of L6 myotubes was tested.

The procedure for the synthesis of 1-*O*- α -methyl-D-glucopyranoside¹³ was used to obtain 1-*O*- α -methyl-D-xylopyranoside (**1**) by interacting D-xylose, instead of D-glucose, with methanol in the presence of Dowex 50. 1,2-*O*-Isopropylidene- α -D-xylofuranose, which was the starting material for the synthesis of 2-*O*- α,β -methyl-D-xylopyranose (**2**), 3-*O*- α,β -methyl-D-xylopyranose (**3**), and 5-*O*- α,β -methyl-D-xylofuranose (**4**), was synthesized according to Moravcova et al.¹⁴ This one-step reaction between D-xylose and acetone results in an isopropylidene addition to the glycosylic and second hydroxyl positions in D-xylose, leaving the third and fifth hydroxyl groups available for chemical manipulations. The synthesis of **2** was carried according to Bowering¹⁵ by interacting 1,2-*O*-isopropylidene- α -D-xylofuranose with benzyl bromide in the presence of potassium hydroxide. The resulting 3,5-*O*-dibenzyl-1,2-*O*-isopropylidene- α -D-xylofuranose was subjected to a HCl(g)-induced hydrolysis to remove the isopropylidene ring, followed by methylation of the glycosylic position, as described above

Scheme 1. Synthesis of **7**^a



^a Reagents and conditions: (a) 2-methoxypropene, dry DMF, 5 M HCl in methanol (catalytic amount), 4 °C, 1.5 h; (b) methyl iodide, Ag₂O, DMF, room temperature, 24 h; (c) acetic acid, 2 M H₂SO₄ in water, 100 °C, 24 h.

for **1**. The hydroxyl group in position 2 was then interacted with methyl iodide in the presence of Ag₂O to produce 1,2-*O*-dimethyl-3,5-*O*-dibenzyl- α -D-xylofuranoside. Compound **2** was obtained by the removal of the benzyl moieties by hydrogenation and demethylation of the glycosylic position by acid-catalyzed hydrolysis. The synthesis of **3** was performed according to Levine and Raymond¹⁶ by interacting 1,2-*O*-isopropylidene- α -D-xylofuranose in dry pyridine with benzoyl chloride, which reacts with the primary alcohol in the fifth position, to produce 5-*O*-benzoyl-1,2-*O*-isopropylidene- α -D-xylofuranose. The hydroxyl group in the third position remained free to interact with methyl iodide to produce 5-*O*-benzoyl-3-*O*-methyl-1,2-*O*-isopropylidene- α -D-xylofuranose. Following the removal of the benzoyl moiety with barium oxide and the isopropylidene ring by acid hydrolysis, **3** was obtained. The principles of the procedure of Levine and Raymond¹⁶ were also used for a selective methylation of the fifth position in D-xylose to produce **4**. Briefly, 1,2-*O*-isopropylidene- α -D-xylofuranose was interacted with *p*-toluenesulfonyl chloride in dry pyridine to obtain 5-*O*-tosyl-1,2-*O*-isopropylidene- α -D-xylofuranose. Treatment with sodium methoxide exchanged the tosyl moiety with a methyl group, and acid hydrolysis removed the isopropylidene ring to obtain **4**.

Scheme 1 depicts the novel synthesis of 4-*O*- α,β -methyl-D-xylopyranose (**7**). Briefly, 1-*O*- α -methyl-2,3-isopropylidene-D-xylopyranoside (**5**) was synthesized from **1** according to the synthetic strategy described by Takeo et al.¹⁷ The hydroxyl group in the fourth position of **5** was methylated as described above for **3**. The resulting compound, 1-*O*- α -methyl-4-*O*-methyl-2,3-isopropylidene-D-xylopyranoside (**6**), was subjected to an acid-catalyzed hydrolysis to remove the protection groups and obtained **7**.

Compounds **2**, **4**, and **7**, used at concentrations as high as 20 mM for up to 48 h incubations, had no marked effect on hexose transport in L6 myotubes (Supporting Information Table 2). Figure 3 shows that **1** and **3** (5 mM each) were more potent than D-xylose (20 mM) in increasing the rate of hexose uptake (1.98 ± 0.08 - and 2.10 ± 0.16 -fold, respectively, in comparison with the 1.49 ± 0.07 -fold increase of D-xylose). Moreover, the effects of D-xylose, **1**, and **3** were additive to the hexose transport-enhancing effect of insulin.

In general, the QSAR analyses indicated that positions 2, 4, and 5 in D-xylose are critical for its biological activity and that methylation of positions 1 and 3 not only conserved activity but rendered the derivatives more efficacious and potent than D-xylose.

The unexpected finding that 1-*O*- and 3-*O*-methylation augments considerably the hexose transport capacity of the resulting molecules in comparison with D-xylose could imply that longer alkyl substitutions at these two positions further improve their potency and efficacy. However, 1-*O*- α,β -ethyl-D-xylopyranoside (**8**)¹⁸ failed to modulate hexose transport in myotubes, indicating that elongation of the alkyl group at the

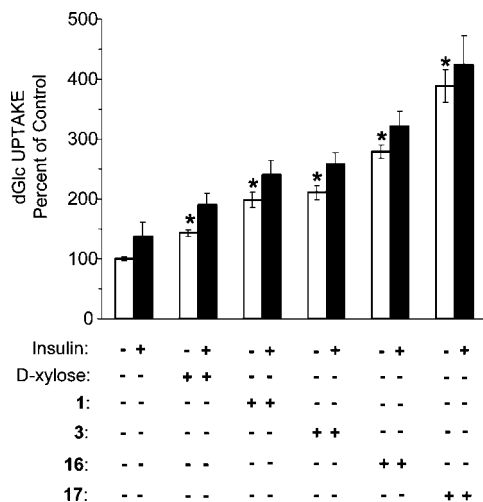


Figure 3. Effects of D-xylose, **1**, **3**, **16**, and **17** on hexose uptake in L6 myotubes. Myotube cultures were washed and received fresh α MEM containing 23.0 mM D-glucose and 20.0 mM D-xylose or 5.0 mM **1**, **3**, **16**, or **17** and incubated for 7 h. Insulin effect was measured as described in the Experimental Section. The basal rate of dGlc uptake (1.32 ± 0.05 nmol (mg of protein) $^{-1}$ min $^{-1}$) was taken as 100%. *, $p < 0.05$ in comparison with the respective 23.0 mM glucose control.

glycosyl position was disadvantageous. Ethyl (**16**), propyl (**17**), and *n*-butyl (**18**) substitutions at position 3 in D-xylose were performed as described in Scheme 2: 1,2-*O*- α -isopropylidene-D-xylofuranose was interacted with trityl chloride to produce 5-*O*-trityl-1,2-*O*- α -isopropylidene-D-xylofuranose (**9**).¹⁹ Following its alkylation with ethyl iodide, propyl iodide, or *n*-butyl iodide in the presence of Ag₂O and removal of the trityl and isopropylidene protective groups by acid catalysis, the corresponding 3-*O*-alkyl-D-xylopyranoses (**16**, **17**, and **18**) were obtained.

Figure 3 shows that **16** and **17** increased the rate of hexose transport in myotubes 2.79 ± 0.11 - and 3.89 ± 0.27 -fold above the basal uptake level, whereas **18** was inactive (Supporting Information Table 2). Similar to D-xylose, **1**, and **3**, the effects of **16** and **17** were additive to the effect of insulin. These data indicate that a 3C alkyl elongation at position 3 of D-xylose was optimal. Nevertheless, although the efficacy of **16** and **17** was improved in comparison with **1** and **3**, their potency remained modest (2.0 and 5.0 mM for half-maximal and maximal effects, respectively).

Effects of Lipophilic Derivatives of D-Xylose. A common method to improve the pharmacokinetic parameters of hydrophilic molecules, such as D-xylose, **16**, or **17**, is to synthesize active lipophilic derivatives that readily diffuse into cells through the lipid phase of the plasma membrane and act intracellularly, thus yielding long-acting and more potent and efficacious derivatives than the parent compound.²⁰ Often, such derivatives are prodrugs, which are activated *in vivo* by spontaneous or enzymatic dissociation of the lipophilic substituents. On the basis of the QSAR data we planned D-xylose glycoside derivatives and derivatives in which positions 2, 4, and 5 were maintained intact or bound to dissociable groups. In line with this strategy, we synthesized and screened various glycoside-, ester-, phosphate ester-, ketal-, and ether bond-based derivatives of these positions in D-xylose. The synthetic procedures, effects in the hexose uptake assay, and cytotoxicity of these compounds are presented in the section on inactive D-xylose derivative in the Supporting Information. Most of these compounds had no effect on the hexose transport capacity in the myotubes. We hypothesize that some of these derivatives are subjected to rapid and

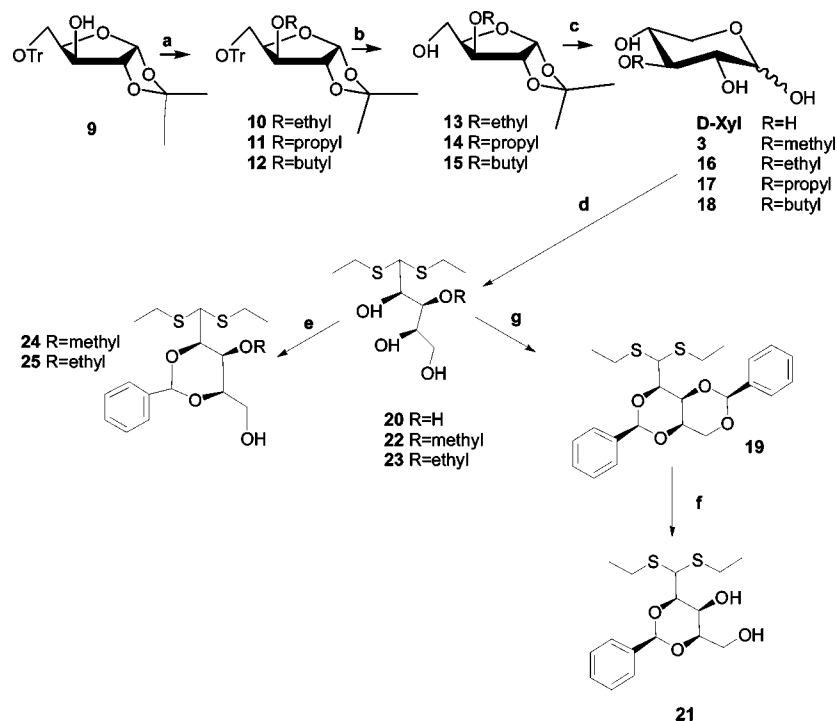
efficient enzymatic degradation either in the culture medium or intracellularly, whereas the cell membrane permeability of others might be impeded.

In contrast to these inactive derivatives, dithioether addition to the glycosyl position combined with acetal substitutions at positions 2,4 and/or 3,5 produce potent and long-acting derivatives. It has been shown that thioether bonds in xenobiotics are oxidized by the cytochrome P450 system to release the core compound and sulfoxide.²¹ In addition, Nomura et al. showed that cyclic acetal substitutions on D-ribose moieties were effectively reduced under physiological conditions, releasing the intact pentose.²² The compound 2,4:3,5-dibenzylidene-D-xylose diethyl dithioacetal (**19**) was synthesized according to Curtis and Jones²³ (Scheme 2). Briefly, D-xylose was converted to D-xylose diethyl dithioacetal (**20**) by reaction with ethanediol in the presence of concentrated HCl. Benzaldehyde was interacted with **20** in the presence of HCl(g), and the resulting **19** was then crystallized from ethanol. 2,4-Benzylidene-D-xylose diethyl dithioacetal (**22**) was prepared by a selective acid hydrolysis of the 3,5-acetal ring in **19** as described²⁴ (Scheme 2). Briefly, **19** was dissolved in an ice-cold mixture of chloroform:methanol:water (42:56:2) and a catalytic volume of concentrated HCl. Following stirring at 4 °C for 3 days, three products were obtained: **20**, **21**, and 3,5-benzylidene-D-xylose diethyl dithioacetal. Compound **21** was purified by PLC (using diethyl ether as the eluent), extracted with chloroform, and crystallized with petroleum ether:diethyl ether (40:60).

Since the addition of an alkyl group in position 3 of D-xylose improved both the efficacy and potency of the molecule, we also synthesized 3-*O*-alkyl derivatives of **21**. Scheme 2 also shows the synthesis of the 3-*O*-methyl- and 3-*O*-ethyl derivatives (**24** and **25**). Dithioacetal derivatives at the glycosyl position of **3** and **16** were prepared by coupling with ethanethiol employing an acidic catalysis to produce the corresponding **22** and **23**. Selective 2,4-benzaldehyde acetal ring addition to these compounds, using benzaldehyde dimethyl acetal under dry conditions and gentle acid catalysis, produced **24** and **25**. The chirality of carbon atoms in the D-xylose backbone in **19**, **21**, and **24** is maintained. In **19** two additional chiral centers were introduced in the 2,4- and 3,5-benzylidene rings. According to Rao and Grindley²⁵ the conformations of the benzylidene carbon atom in **19** are 2,4(*R*) and 3,5(*S*) while in **21** it is 2,4(*R*). The synthetic procedures of **24** and **25** produced a mixture of *S/R* stereoisomers in position 2,4 (46:54 and 39:61, respectively).

Compounds **19**, **21**, and **24** increased the rate of hexose transport in L6 myotubes in a time-dependent manner; **21** and **24** peaked at 7 h while **19** peaked at 18 h, after which a gradual decline was observed (Figure 4A). The concentrations used in this experiment were based on the dose-response analysis (Figure 4B), in which maximal stimulatory effects of **19**, **21**, and **24** were observed at 5, 150, and 50 μ M, respectively.

The methyl ether substitution at position 3 in **24** augmented its potency 3-fold compared to that of **21**. Interestingly, an ethyl ether substitution at this position rendered **25** inactive (Supporting Information Table 2). Of major interest is the finding that the potency of **19** was 30- and 10-fold higher than those of **21** and **24**, respectively. The high lipophilicity of **19** (calcd log $P = 4.99$)²⁶ correlates well with this enhanced potency, in contrast to the significantly lower log P values of **21**, **24**, and obviously D-xylose (2.40, 2.80, and -0.83, respectively). It is important to note that we used 10% rather than the usual 2% (v/v) FCS in the medium culture of mature myotubes to improve the solubility of **19**. We measured the protein binding capacity of **21** in this high-serum culture medium, as described in the

Scheme 2. Synthesis of 3-Alkyl and Benzylidene Derivatives of D-Xylose^a

^a Reagents and conditions: (a) respective alkyl iodide, Ag₂O, DMF, room temperature, 24 h; (b) TFA, chloroform; (c) 0.1% H₂SO₄, water, 80 °C, 2 h; (d) ethanethiol, cold HCl, overnight, room temperature; (e) benzaldehyde dimethyl acetal, molecular sieve, 3 Å, dry DMF, dry HCl in dioxane, room temperature, overnight; (g) benzaldehyde, dry HCl gas, 20 min, ice bath; (f) chloroform/methanol/water (15:20:0.75), HCl, 4 °C, 3 days.

Experimental Section, and found it to be $98.0 \pm 0.3\%$. Thus, when the total (added) concentration of **19** in the culture medium was $5 \mu\text{M}$, its calculated free (non-protein-bound) concentration was nearly 100 nM . Of importance are the findings that the viability of myotubes was not compromised on the presence of **19**, **21**, **24**, or D-xylose under the incubation conditions described above (Supporting Information Figure 2).

Another aspect of the higher lipophilicity of **19** in comparison to **21** and **24** is depicted in Figure 4C: L6 myotubes were treated with optimal concentrations of these derivatives and of D-xylose. At the times of respective peak effects, the cultures were washed thoroughly, received fresh medium with 23.0 mM D-glucose, and the rate of hexose transport was determined thereafter. These data were used to calculate the half-life of the effect of the test compounds after washing. A positive correlation between log *P* values and half-life values was revealed (inset to Figure 4C). The emerging rank order, D-xylose < **21** < **24** < **19**, supports the view that the extended duration of action of **19** results from its higher lipid solubility in cells. Worth mentioning is the observation that **19**, **21**, and **24** were active in the absence of insulin and that their effects were additive to that of the hormone when incubated together (Figure 4D), suggesting that the mechanisms of action of these synthetic compounds and insulin are distinct.

To be of relevance for diabetes treatment, these compounds should be effective also in nontransformed human muscle cells. This was indeed the case (Figure 4E): primary cultures of human myotubes exposed to D-xylose, **19**, **21**, or **24** increased significantly the rate of hexose transport (1.43 ± 0.15 -, 1.59 ± 0.18 -, 1.49 ± 0.12 -, and 1.40 ± 0.17 -fold, respectively, over the control level).

Mechanism of Action of D-Xylose, 19, 21, and 24. The temporal characteristics of the hexose transport-augmenting effects of insulin and of D-xylose and its derivatives differ

greatly. While insulin acts within minutes and its effect disappears shortly after its removal, the onset and off rates of the effects of D-xylose, and especially of its lipophilic derivatives, are long and positively correlated with the lipophilicity of the compounds. Nevertheless, the end point effects of insulin, D-xylose, and its lipophilic derivatives on the muscle-specific glucose transporter GLUT4 are similar: Panels A and B of Figure 5 show that insulin, D-xylose, and the derivatives increased the abundance of GLUT4myc, but not of GLUT1myc, in the plasma membrane of L6 myotubes. However, the effect of insulin on GLUT4myc abundance in the plasma membrane of myotubes was fast (30 min) whereas several hours were required for D-xylose, **19**, **21**, and **24** to exert their maximal effects (7 h of incubation for all except 18 h for **19**). These treatments did not alter the total cell content of GLUT1 or GLUT4, as was determined in whole cell lysates of myc epitope-tagged L6 myotubes (Figure 5) or wild-type L6 myotubes (Supporting Information Figure 3).

The experimental conditions of the standard hexose uptake and the colorimetric determination of surface GLUT1myc and GLUT4myc differ greatly: the former is short and carried at room temperature, while the latter is longer and entails extensive washes in a buffer containing goat serum at 4 °C. Therefore, to correlate plasma membrane GLUT1myc and GLUT4myc data to hexose transport levels, we also determined the rate of [³H]dGlc uptake in wild-type and in GLUT4myc- and GLUT1myc-tagged L6 myotubes under the experimental conditions employed in the colorimetric assay (except for the fixation stage; the uptake period at 4 °C was 15 min). The relative effects of low and high glucose concentrations, insulin, D-xylose, and **19**, **21**, and **24** were similar to those observed under conditions of the standard uptake assay (Supporting Information Figure 4). Thus, the changes found in plasma membrane abundance of

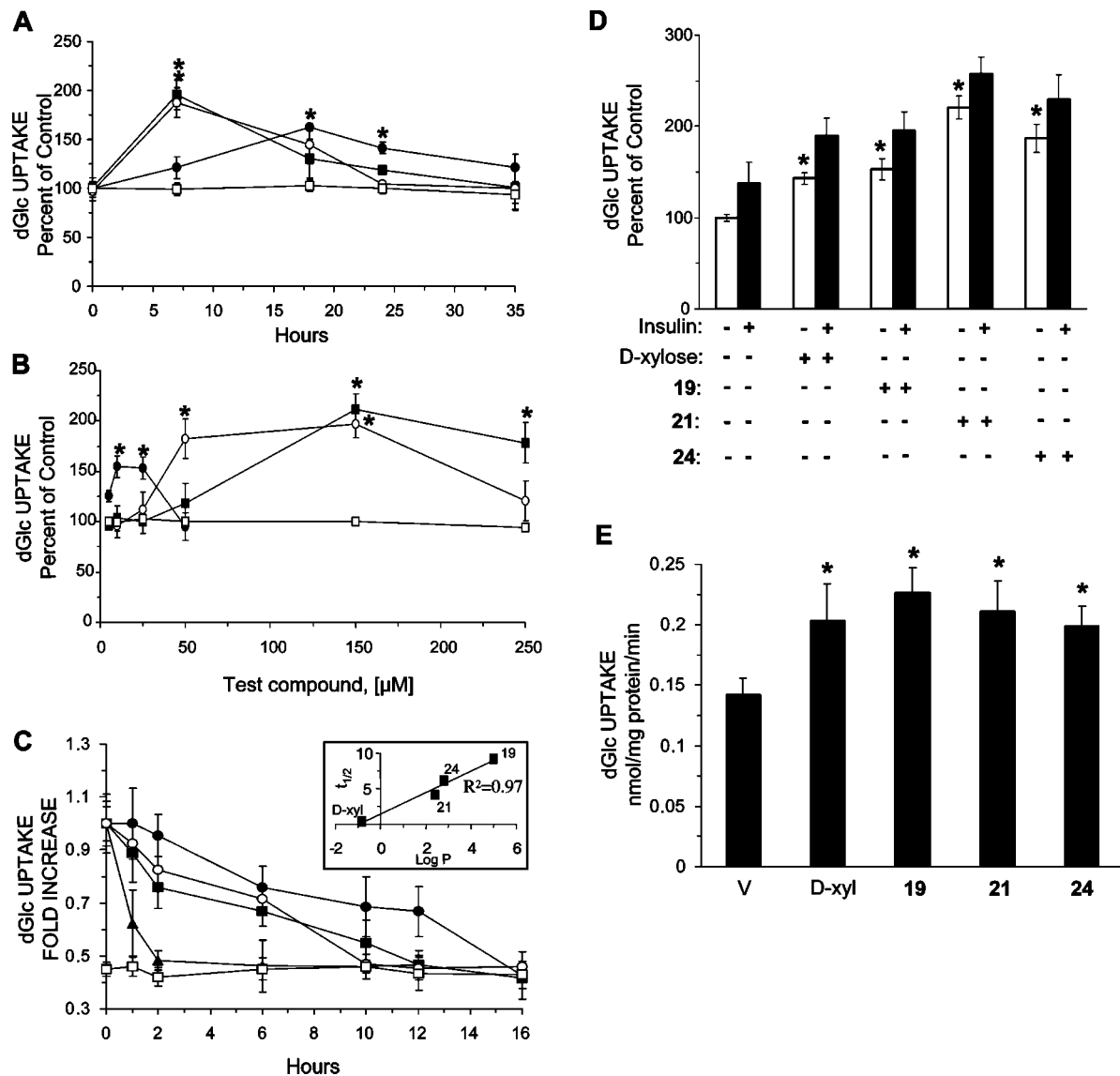


Figure 4. Compounds **19**, **21**, and **24** increase the rate of hexose uptake in L6 myotubes and human skeletal muscle myotubes. (A) Time-course analysis. Myotube cultures were washed and received fresh medium supplemented with 10% (v/v) FCS, 23.0 mM D-glucose, and 5 μ M **19** (●), 150 μ M **21** (■) or 50 μ M **24** (○). Control myotubes received the vehicle (V) only (□). After incubation for the indicated time periods the cultures were taken for the dGlc uptake assay. The basal rate of uptake at zero time (1.17 ± 0.09 nmol of dGlc (mg of protein) $^{-1}$ min $^{-1}$) was taken as 100%. (B) Dose–response analysis. Myotube cultures were incubated with medium supplemented with 10% (v/v) FCS, 23.0 mM D-glucose, and increasing concentrations of **19** (●, 7 h), **21** (■, 18 h), or **24** (○, 7 h). Control myotubes received the vehicle only (□) and were incubated for 18 h. The cultures were then washed and taken for the standard [3 H]dGlc uptake assay. The basal rate of dGlc uptake at zero time (1.58 ± 0.21 nmol (mg of protein) $^{-1}$ min $^{-1}$) was taken as 100%. (C) Myotube cultures were exposed to D-xylose, **19**, **21**, and **24** as described for (A). The cultures were then washed at the respective peak times depicted in (B) and received fresh medium supplemented with 23.0 mM D-glucose. The rate of dGlc uptake was assayed at the indicated times. Inset: Correlation between log *P* values of D-xylose, **19**, **21**, and **24** and their half-maximal hexose uptake augmenting capacity. (D) Combined effects of **19**, **21**, and **24** and of insulin. The cultures were treated as described above and incubated for 24 h. The basal rate of dGlc uptake at zero time (1.13 ± 0.06 nmol (mg of protein) $^{-1}$ min $^{-1}$) was taken as 100%. (E) Human skeletal muscle myotubes were prepared as described in the Experimental Section. The cultures were treated with **19**, **21**, and **24** as described above for (C) and taken for the standard [3 H]dGlc uptake assay. *, *p* < 0.05, in comparison with the respective 23.0 mM glucose control.

GLUT4myc reflected the changes in the hexose transport capacity of myotubes.

Since D-xylose and its derivatives increased the plasma membrane GLUT4 content like insulin, it was questioned whether they activated the insulin signaling pathways, including PI3-kinase and its downstream effector protein kinase B (Akt/PKB).²⁷ Inhibition of PI3-kinase or Akt/PKB silences the insulin transduction pathway;²⁸ we therefore postulated that if D-xylose derivatives act through this pathway, their effects on glucose transport would be abolished by wortmannin that inhibits PI3-kinase²⁹ and by the commercially available inhibitor of Akt/PKB (1,3-dihydro-1-(1-((4-(6-phenyl-1*H*-imidazo[4,5-*g*]quinox-

alin-7-yl)phenyl)methyl)-4-piperidinyl)-2*H*-benzimidazol-2-one trifluoroacetate salt hydrate).³⁰ Panels A and B of Figure 6 show the expected abolishment of insulin-stimulated hexose uptake in L6 myotubes by inhibiting PI3-kinase and Akt/PKB. In contrast, the hexose transport-stimulatory effects of D-xylose, **19**, **21**, and **24** remained intact in the presence of these inhibitors, indicating that neither PI3-kinase nor Akt/PKB participates in this action. Further support for this conclusion came from the determination of the extent of Ser⁴⁷³ and Thr³⁰⁸ phosphorylation in Akt/PKB: Figure 6C depicts the predictable insulin-induced phosphorylation of both moieties in Akt/PKB.²⁷ D-xylose, **19**, **21**, and **24** had no comparable phosphorylating capacity, except

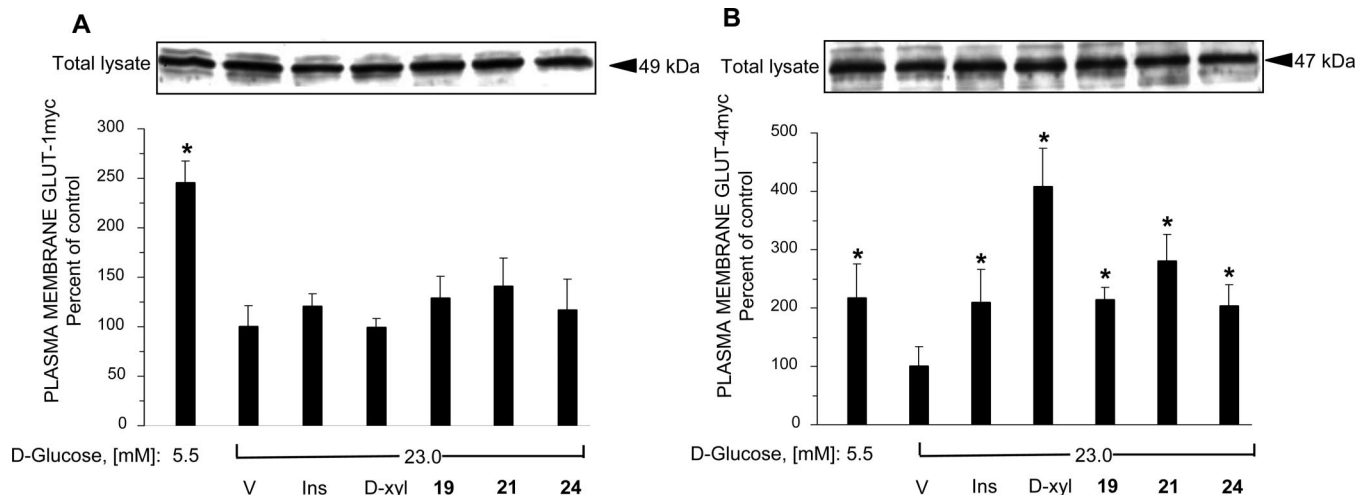


Figure 5. D-Xylose, **19**, **21**, and **24** increase the abundance of GLUT4, but not GLUT1, in the plasma membrane of L6 myotubes. Myotubes expressing GLUT1myc and GLUT4myc were preconditioned with the indicated glucose levels and then received the vehicle (V) or 200 nM insulin, 20 mM D-xylose, 5 μ M **19**, 150 μ M **21**, or 50 μ M **24**, as described for Figure 4B. At the end of incubation, the cultures were taken for immunodetection of surface GLUT1myc (A) or GLUT4myc (B), as described in the Experimental Section. The Western blots depict the total cell content of the corresponding glucose transporters in whole cell lysates. *, $p < 0.05$, in comparison with the control (V).

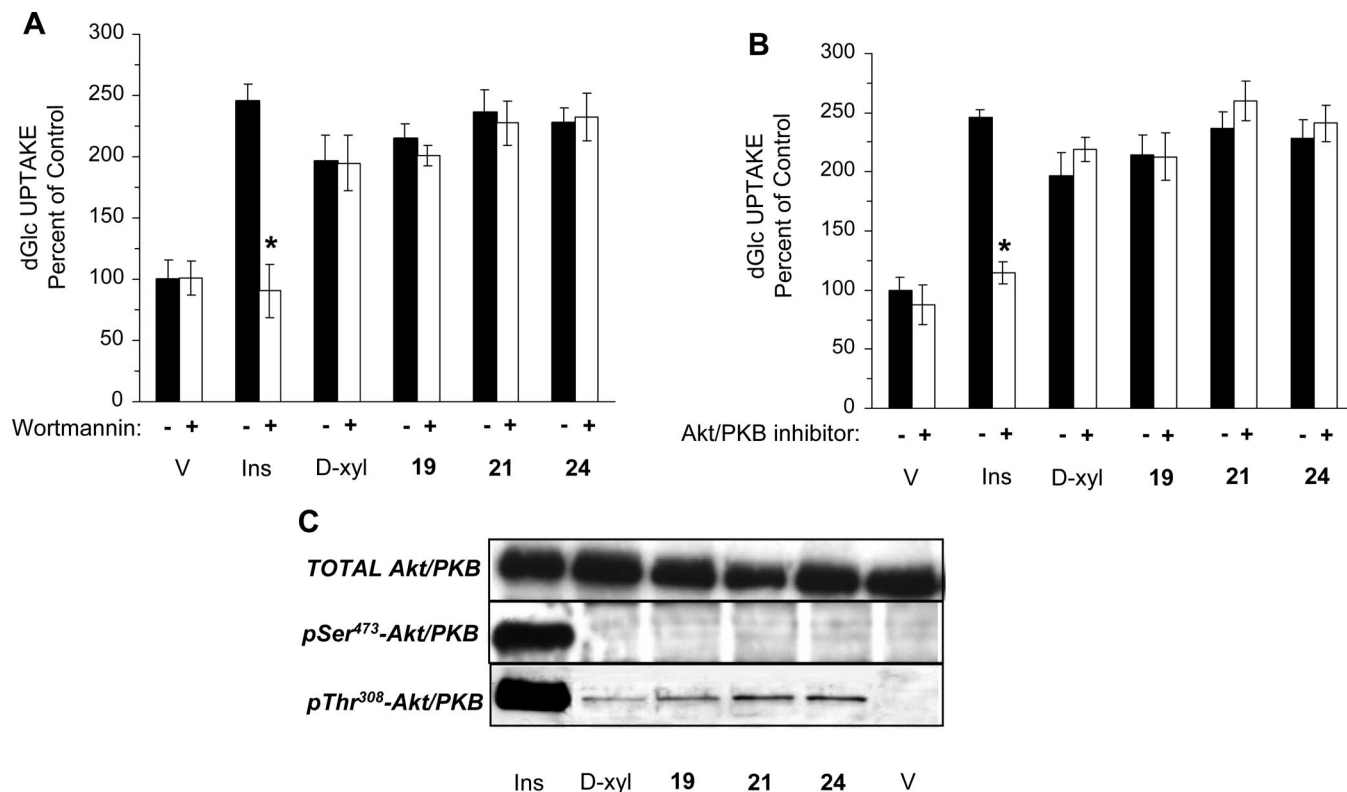


Figure 6. D-Xylose and **19**, **21**, and **24** augment the rate of hexose transport in L6 myotubes in a PI3K- and Akt/PKB-independent manner. Myotube cultures were washed and received fresh medium containing the same D-glucose concentration and 20 mM D-xylose, 5 μ M **19**, 150 μ M **21**, 50 μ M **24**, or the vehicle (V) in the absence or presence of 100 nM wortmannin (A) or 100 nM Akt/PKB inhibitor (B), as described under Figure 4B. Insulin effect was measured as described in the Experimental Section. Wortmannin or Akt/PKB inhibitor was added 30 min before the addition of test compounds or insulin. The basal rate of dGlc uptake (1.02 ± 0.09 nmol (mg of protein)⁻¹ min⁻¹) in myotubes exposed to 23 mM D-glucose (V) was taken as 100%. *, $p < 0.05$, in comparison with the respective controls. (C) Whole cell lysates were prepared from myotube cultures that were treated with D-xylose, **19**, **21**, and **24** as described above. Western blot analyses were performed with antibodies against PKB, pThr³⁰⁸-PKB, and pSer⁴⁷³-PKB, as described in the Experimental Section and Supporting Information Table 3.

for a very weak phosphorylation of Thr³⁰⁸. We doubt that the latter plays a role in mediating the effect of D-xylose derivatives since, as suggested by Bouzakri et al.,³¹ the phosphorylation of Ser⁴⁷³, but not of Thr³⁰⁸, is imperative for insulin-induced stimulation of glucose uptake in skeletal muscles. Therefore, our findings strongly imply that D-xylose, **19**, **21**, and **24** do

not recruit Akt/PKB for transducing their hexose transport-stimulatory effects.

The translocation of GLUT4 to the plasma membrane of skeletal muscle is also mediated by non-insulin-dependent stimuli, such as muscle contraction and reduced energy charge that activate 5-AMP-activated kinase (AMPK α)⁵. Figure 7A

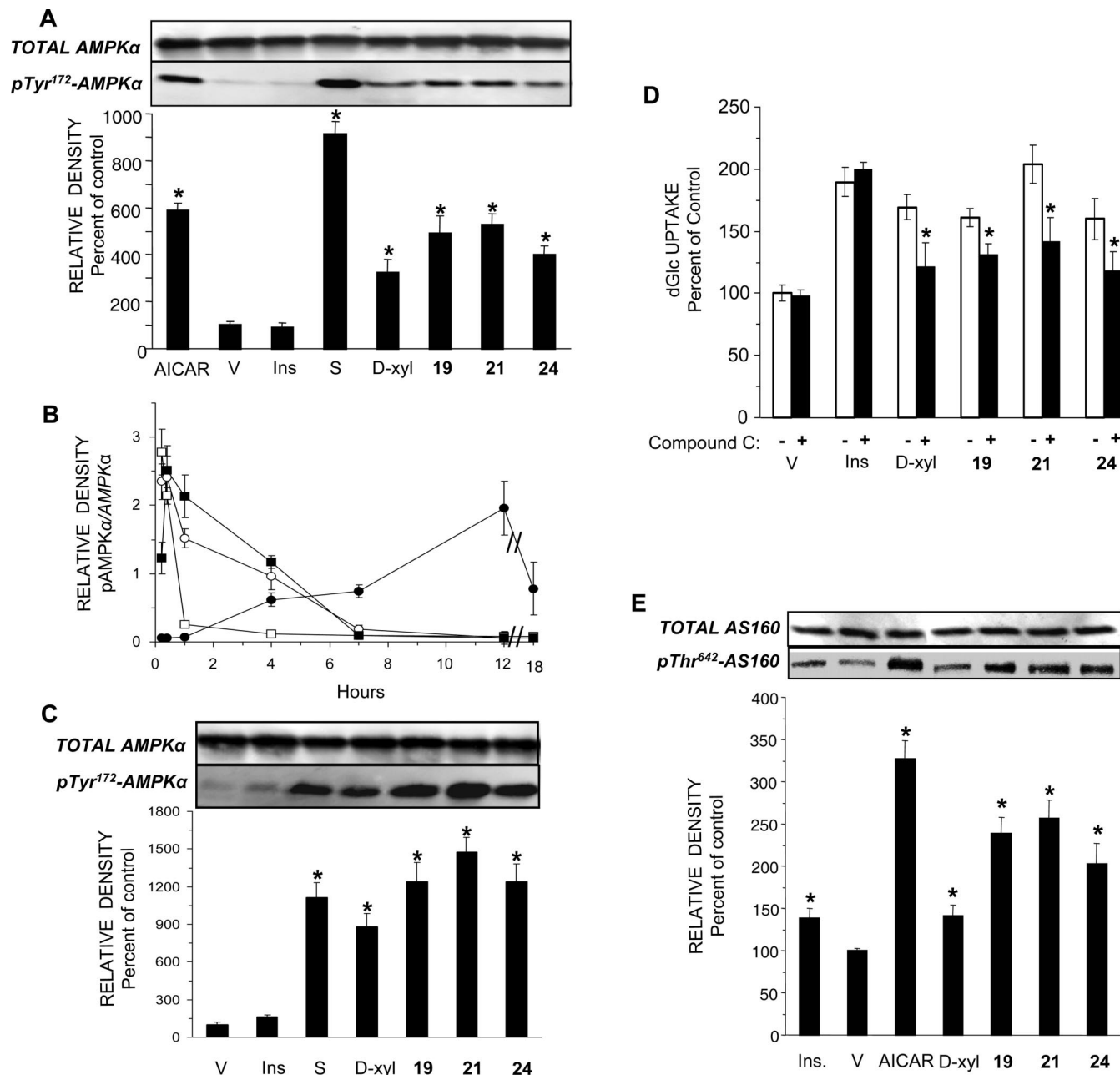


Figure 7. D-Xylose, **19**, **21**, and **24** activate AMPK α and AS160. (A) Myotube cultures were treated with D-xylose (D-xy), **19**, **21**, **24**, insulin (Ins), or the vehicle (V) as described in the legend to Figure 4A. AICAR (4 mM) and D-sorbitol (S, 0.25 M) were present for 1 h and 30 min, respectively. Whole cell lysates were prepared, and Western blot analyses were performed with antibodies against AMPK α and pTyr¹⁷²-AMPK α . (B) Time-dependent phosphorylation of Tyr¹⁷²-AMPK α . The experiment was performed as described in (A). The incubation was terminated at the indicated times, and the myotubes were lysed and taken for Western blot analyses of AMPK α and pTyr¹⁷²-AMPK α . (C) Human myotubes were treated as described above for (A) and taken for Western blot analysis of AMPK α and pTyr¹⁷²-AMPK α . (D) The cultures were preincubated for 1 h with 5 μ M Compound C prior to the addition of D-xylose (D-xy), **19**, **21**, or **24**. The basal rate of dGlc uptake (1.45 \pm 0.09 nmol (mg of protein)⁻¹ min⁻¹) in myotubes exposed to the vehicle was taken as 100%. (E) Whole cell content of AS160 and pThr⁶⁴²-AS160 was determined by Western blot analysis in samples that were prepared as described above for (A). Representative blot and a summary of $n = 3$. *, $p < 0.05$, in comparison with the respective controls.

shows that the classical AMPK α activators AICAR³² and a hyperosmolar shock (0.25 M D-sorbitol),³³ but not insulin, induced significant Tyr¹⁷² phosphorylation in AMPK α in L6 myotubes. D-Xylose, **19**, **21**, and **24** significantly induced Tyr¹⁷² phosphorylation (3.23 \pm 0.57-, 4.89 \pm 0.77-, 5.25 \pm 0.49-, and 3.98 \pm 0.38-fold above control, respectively), whereas total cell content of AMPK α was not altered in their presence. These effects of D-xylose and its derivatives on AMPK α phosphorylation were time-dependent (Figure 7B): Peak effects were obtained at 1–2 h for D-xylose, **21**, and **24** and at 12 h for **19**, demonstrating that the activation of AMPK α precedes the

maximal stimulation of hexose transport. Again, a similar positive correlation between the onset of the stimulatory effects and log P values of these compounds is apparent (Figure 4C). D-Xylose-, **19**-, **21**-, and **24**-induced phosphorylation of Tyr¹⁷² in AMPK α was also evident in primary cultures of human skeletal muscles (Figure 7C).

We also used Compound C, a selective inhibitor of AMPK α ,³⁴ to evaluate directly the role of AMPK α in mediating the action of D-xylose, **19**, **21**, and **24**. Compound C (5 μ M) significantly impeded the ability of D-xylose and its derivatives to augment the rate of hexose transport in L6 myotubes (Figure

Table 1. ATP Content Is Not Altered in L6 Myotubes Following Treatment with D-Xylose, **19**, **21**, or **24**^a

| condition | ATP (mmol/mg of protein) |
|------------------------|--------------------------|
| 5.0 mM D-glucose (L) | 1.84 ± 0.09 |
| 23.0 mM D-glucose (H) | 1.94 ± 0.08 |
| H + insulin (100 nM) | 1.66 ± 0.10 |
| H + DMSO (1.0%) | 1.90 ± 0.06 |
| H + D-xylose (20 mM) | 1.60 ± 0.03 |
| H + 19 (5 μM) | 1.99 ± 0.12 |
| H + 21 (150 μM) | 1.73 ± 0.08 |
| H + 24 (50 μM) | 1.69 ± 0.05 |
| H + DNP (5 mM, 10 min) | 0.72 ± 0.08 ^b |

^a L6 myotubes were preconditioned with the indicated glucose concentration and treated with the various compounds as described in the legend to Figure 5. At the end of incubation the myotubes were lysed, and the ATP content was determined as described in the Experimental Section. ^b $p < 0.05$, in comparison with the 23.0 mM D-glucose (H) incubation. L, low (5.0 mM D-glucose); H, high (23.0 mM D-glucose).

7D): 68.9 ± 10.7%, 48.8 ± 3.4%, 60.0 ± 8.1%, and 69.2 ± 8.6% reduction, respectively ($p < 0.05$), in comparison with the respective control cells. Table 1 shows that D-xylose, **19**, **21**, and **24** activate AMPK α in an adenosine-independent manner because total cell ATP content in L6 myotubes was not altered significantly in their presence. The uncoupler DNP (5 mM, 10 min), which reduced significantly the ATP content, served as a positive control.

The protein AS160 mediates insulin-stimulated GLUT4 translocation in myotubes following the activation of Akt/PKB. Equally important, AS160 is also activated under conditions of AMPK α stimulation.³⁵ We therefore determined the extent of Thr⁶⁴² phosphorylation in AS160, a marker of its activation, in L6 myotubes treated with insulin and with D-xylose, **21**, **22**, and **25**. Figure 7E shows that, in concert with the stimulation of the rate of hexose transport and AMPK α phosphorylation, these treatments elicited significant Thr⁶⁴² phosphorylation in AS160.

In summary, this study shows that high levels of D-xylose increase the rate of hexose transport in L6 myotubes by increasing the plasma membrane content of GLUT4 in an AMPK α -dependent manner. Interestingly, AMPK α is considered a key target for the development of new pharmaceuticals to treat obesity, type 2 diabetes, and the metabolic syndrome.⁵ For instance, recent studies have linked the blood glucose lowering effects of the antihyperglycemic drug metformin (1,1-dimethylbiguanide) to the activation of AMPK α .^{36,37} Lipophilic derivatives of D-xylose were synthesized to overcome the poor pharmacokinetic and pharmacodynamic parameters of D-xylose. The highly lipophilic **19**, **21**, and **24** exerted significant hexose transport-stimulatory effects at low concentrations in rat and human cultured myotubes in an AMPK α -dependent manner. It is assumed that these compounds act as prodrugs and release the active parent compound upon intracellular oxidation of the thioether group and the reduction of the acetal substitutions.

These findings emphasize the great potential of this and similar compounds in the development of novel potent and long-acting antihyperglycemic compounds. Thus, future syntheses and criteria for development of such D-xylose derivatives need to be based on selection of suitable dissociable lipophilic moieties to be coupled to the core molecule, the lipophilicity and membrane permeability of the derivatives, the intracellular release of the parent molecule, and its potential to activate AMPK α to increase the cell surface abundance of GLUT4 in skeletal muscles.

Experimental Section

Materials. D-Arabinone, 2,4-dinitrophenol (DNP), 2-deoxy-D-glucose, D-glucose, D-lyxose, 3-O-methyl-D-glucose, 3-O-methyl-

D-xylose, D-ribose, L-glucose, 1-O-methyl- β -D-xylopyranoside, AICAR (5-aminoimidazole-4-carboxamide-1- β -ribofuranosyl 5- β -monophosphate), Akt/PKB (Akt1/2 kinase) inhibitor, BSA (bovine serum albumin, fraction V), chloroform-*d*, D₂O, dimethyl sulfoxide-*d*₆, Igepal CA-630, *O*-phenylenediamine (OPD), and wortmannin were purchased from Sigma Chemical Co (St. Louis, MO). Anhydrous acetonitrile and dry DMF were also from the same supplier and used as received. D-Sorbitol was from BDH (Poole, U.K.). Compound C was from Calbiochem (Darmstadt, Germany). American Radiolabeled Chemicals (St. Louis, MO) supplied 2-[1,2-³H(N)]deoxy-D-glucose (2.22 TBq/mmol), 3-*O*-[methyl-³H]-D-glucose (2.22 TBq/mmol), [¹⁴C-(U)]sucrose (22.2 GBq/mmol), and [1-¹⁴C]-D-xylose (2.03 GBq/mmol). The following antibodies were used: anti-AMPK α and anti-pThr¹⁷²-AMPK α from Cell Signaling Technology (Beverly, MA); anti Akt/PKB α (PH domain) and anti pSer⁴⁷³-Akt/PKB α from Upstate Biotechnology (Lake Placid, NY); anti pThr³⁰⁸-Akt1/PKB and anti-C-Myc (A-14) from Santa Cruz Biotechnology (Santa Cruz, CA); and anti AS160 and anti pT⁶⁴²-AS160 from Acris antibodies (Hiddenhausen, Germany). Horseradish peroxidase-conjugated anti-rabbit IgG was from Jackson ImmunoResearch (West Grove, PA). α -Minimal essential medium (α MEM), EZ-ECL chemoluminescence detection kit for HRP, goat serum, fetal calf serum (FCS), L-glutamine, and antibiotics were from Biological Industries (Beth-Haemek, Israel). Preparative silica gel glass plates were from Yoel Naim Ltd. (Rehovot, Israel). Silica gel 60 F₂₅₄ TLC plates were purchased from Merck (Darmstadt, Germany) Organic solvents (HPLC grade) were purchased from Frutarom Ltd. (Haifa, Israel) and Mallinckrodt Baker B.V. (Deventer, Holland). The boiling range of petroleum ether was 35–60 °C.

Chemical Procedures. Dry pyridine was prepared via reflux with potassium hydroxide for 5 h followed by distillation. Dry methanol was prepared by reflux (8 h) with magnesium and small amount of iodine crystals followed by distillation. Dry dichloromethane was prepared via reflux with P₂O₅ for 12 h followed by distillation. Melting points were determined using a Melting Point SMP apparatus (Stuart Scientific, Stone, Staffordshire, U.K.). Elemental analysis was performed in the Microanalysis Laboratory of the Institute of Chemistry, Faculty of Life Sciences, The Hebrew University (Jerusalem, Israel). Proton and carbon NMR spectra of compounds were obtained with a Varian VXR-300 (300 MHz) spectrometer equipped with a 5 mm probe, and data were processed using VNMR software. Chloroform-*d*, D₂O, and dimethyl sulfoxide-*d*₆ were used as solvents, using tetramethylsilane ($\delta = 0.00$ ppm) as an internal standard. The splitting pattern abbreviations are as follows: s, singlet; d, doublet; t, triplet; q, quartet; m, unresolved multiplet due to the field strength of the instrument; ds, doublet of singlet; *a*, axial; *e*, equatorial position. Electrospray ionization mass spectrometry was measured on a Thermo Quest Finnigan LCQ-Duo (Fisher Scientific, Waltham, MD) in the positive ion mode. In most cases, elution was performed in a 20:79:1 water:methanol:acetic acid mixture at a flow rate of 15 μ L/min. Data were processed using ThermoQuest Finnigan's Xcalibur Biomass Calculation and Deconvolution software. For purification we employed flash column chromatography on Merck silica gel 60 (particle size 230–400 mesh) using dichloromethane and methanol, at various ratios, as eluent. Purification on HPLC (Gilson, Middleton, WI) was performed on C18 preparative and semipreparative columns (Beckman Ultrasphere ODS column, 250 mm \times 10 mm i.d., 5 μ M, and Beckman Ultrasphere ODS column, 250 mm \times 4.6 mm i.d., 5 μ M) using acetonitrile and doubly distilled water in different ratios as the eluent solvent. For analytical TLC silica gel 60 F254 precoated plates (Merck, Darmstadt, Germany) were used, and compounds were visualized with UV light or I₂ vapor.

1-O-Methyl-2,3-O-isopropylidene- α -D-xylopyranoside (5). This compound was synthesized according to the general synthetic procedure described by Takeo et al.¹⁷ with minor modifications: 2-Methoxypropene (6.71 mL) was added dropwise during 15 min to an ice-cold stirred suspension of **1** (5 g) in dry DMF (16 mL) and 5 M HCl in methanol (0.1 mL). The reaction mixture cleared within 10 min and was further stirred for 1 h at room temperature.

Then, 150 mL of chloroform was added, and the solution was extracted three times with 100 mL of water. The resulting organic layer was dried with anhydrous sodium sulfate, filtered, and evaporated to obtain a light brown syrup that was then purified by silica gel chromatography (hexane:ethyl acetate 60:40). After evaporating the organic solvents colorless syrup was obtained. Anal. Calcd for $C_8H_{16}O_5$: C, 52.93; H, 7.90. Found: C, 51.08; H, 7.37. 1H NMR ($CDCl_3$) δ , ppm, 1.54 (ds, 6H, $[CH_3-C-CH_3]$), 3.30 (s, 3H, $[O-C-H_3]$), 3.37 (t, 1H, $[C-H_2]$), 3.41 (d, 1H, $[C-aH_5]$), 3.47 (m, 1H, $[C-H_3]$), 3.83 (m, 1H, $[C-H_4]$), 4.01 (d, 1H, $[C-eH_5]$), 4.84 (d, 1H, $[C-H_1]$).

1,4-O-Dimethyl-2,3-isopropylidene- α -xylopyranoside (6). To a solution of 5 g of **5** in 50 mL of DMF and 4.77 mL of methyl iodide was added gradually 16.6 g of silver oxide (I) during 2 h and then left in the dark at room temperature for 48 h. Then 200 mL of chloroform was added, and the suspension was filtered. The filtrate was washed with 50 mL of chloroform and extracted three times with 100 mL of water. Following drying with anhydrous sodium sulfate, filtering, and evaporating, light brown syrup was obtained. It was purified by silica gel chromatography (ethyl acetate: petroleum ether 20:80) and monitored by TLC (ethanol:diethyl ether 30:70). Colorless syrup was received with a yield of 34.7%. Crystallization attempts were unsuccessful, and the compound was further used as syrup. Anal. Calcd for $C_{10}H_{18}O_5$: C, 55.03; H, 8.31. Found: C, 55.19; H, 7.97. ESMS $[MW + (Na^+)]$ ($C_{10}H_{18}O_5$): *m/e* 241.19, calcd *m/e* 241.12. 1H NMR ($CDCl_3$) δ , ppm, 1.53 (ds, 6H, $[CH_3-C-CH_3]$), 3.34 (t, 1H, $[C-H_2]$), 3.42 (s, 3H, $[O-CH_3]$), 3.49 (s, 3H, $[O-CH_3]$), 3.51 (d, 1H, $[C-aH_5]$), 3.54 (m, 1H, $[C-H_3]$), 3.83 (m, 1H, $[C-H_4]$), 4.1 (d, 1H, $[C-eH_5]$), 4.9 (d, 1H, $[C-H_1]$).

4-O-Methyl- α,β -xylopyranose (7). Compound **6** (1.7 g) was dissolved in 50 mL of hot glacial acetic acid, diluted with 10 mL of boiling 2 M sulfuric acid, and left for 2 h on a steam bath. The mixture then received 10 mL of boiling 2 M sulfuric acid and was similarly heated for an additional 24 h. After the mixture was cooled to room temperature it was mixed with 100 mL of water and neutralized with sodium carbonate. After filtration and lyophilization the white crude mass was extracted with methanol and filtered, and the methanol was evaporated. A remaining yellow syrup was further purified by silica gel short column chromatography (methanol), while monitoring on TLC (methanol:water 90:10). Attempts to crystallize the syrup were unsuccessful. Yield = 77.1%. Anal. Calcd for $C_6H_{12}O_5$: C, 43.90; H, 7.37. Found: C, 43.39; H, 7.21. 1H NMR (D_2O) δ , ppm, 3.31 (t, 1H, $[C-H_2]$), 3.47 (s, 3H, $[O-CH_3]$), 3.51 (d, 1H, $[C-aH_5]$), 3.57 (m, 1H, $[C-H_3]$), 3.88 (m, 1H, $[C-H_4]$), 4.12 (d, 1H, $[C-eH_5]$), (α) 5.29, (β) 4.71 (d, 1H, $[C-H_1]$). ^{13}C NMR (D_2O) δ , ppm, 52.9 (C^4-O-CH_3), 64.9 (C^5), 70.1 (C^3), 76.1 (C^4), 77.5 (C^2), 93.4 (C^1).

5-O-Trityl-3-O-ethyl-1,2-isopropylidene- α -xylopyranoside (10). To an ice-cold solution of 8.3 g of 5-O-trityl-1,2-isopropylidene- α -xylopyranoside (**9**)¹⁹ and 2.5 mL of iodoethane in DMF (50 mL) was added 0.45 g of sodium hydride in three portions. After stirring for 15 min on ice the reaction was left stirring at room temperature for an additional 2 h and then quenched with 30 mL of water and 100 mL of dichloromethane. After separation of layers, the organic phase was washed three times with 100 mL of water, and the common organic phase was dried by anhydrous sodium sulfate and filtered, and the dichloromethane was evaporated. A yellow crystalline mass was obtained and then dissolved in chloroform and purified by silica gel chromatography. The compound was crystallized from ethanol:diethyl ether (5:95) at 4 °C. Yield = 91%; mp 149–154 °C. Anal. Calcd for $C_{29}H_{32}O_5$: C, 75.21; H, 7.32. Found: C, 75.23; H, 7.30. ESMS $[MW + (Na^+)]$: *m/e* 483.19, calcd *m/e* 483.22. 1H NMR ($CDCl_3$) δ , ppm, 1.04 (t, 3H, $[O-CH_2-CH_3]$), 1.51–1.31 (ds, 6H, $[CH_3-C-CH_3]$), 3.86 (q, 2H, $[O-CH_2-CH_3]$), 4.11 (q, 1H, $[C-H_3]$), 4.35 (d, 2H, $[C-H_2]$), 4.55 (q, 1H, $[C-H_2]$), 4.72 (q, 1H, $[C-H_4]$), 5.91 (d, 1H, $[C-H_1]$), 7.10–7.29 (m, 15H, [trityl]).

5-O-Trityl-3-O-propyl-1,2-isopropylidene- α -xylopyranoside (11) and 5-O-Trityl-3-O-butyl-1,2-isopropylidene- α -xylopyranoside (12). These compounds were synthesized as described in the synthetic procedure of **10** using iodopropane or iodobutane,

respectively, instead of iodoethane. Analytical data: **11**, yield = 81%; mp 128–132 °C. Anal. Calcd for $C_{30}H_{34}O_5$: C, 75.81; H, 7.21. Found: C, 75.92; H, 7.22. ESMS $[MW + (Na^+)]$: *m/e* 497.07, calcd *m/e* 497.24. 1H NMR ($CDCl_3$) δ , ppm, 1.05 (t, 3H, $[O-CH_2-CH_2-CH_3]$), 1.28 (q, 2H, $[O-CH_2-CH_2-CH_3]$), 1.51–1.31 (ds, 6H, $[CH_3-C-CH_3]$), 3.88 (q, 2H, $[O-CH_2-CH_2-CH_3]$), 4.21 (q, 1H, $[C-H_3]$), 4.36 (d, 2H, $[C-H_2]$), 4.57 (q, 1H, $[C-H_2]$), 4.72 (q, 1H, $[C-H_4]$), 5.91 (d, 1H, $[C-H_1]$), 7.10–7.29 (m, 15H, [trityl]). **12**, yield = 94%. Anal. Calcd for $C_{31}H_{36}O_5$: C, 75.69; H, 7.13. Found: C, 76.20; H, 7.43. ESMS $[MW + (Na^+)]$: *m/e* 511.31, calcd *m/e* 511.26. 1H NMR ($CDCl_3$) δ , ppm, 1.05 (t, 3H, $[O-CH_2-CH_2-CH_2-CH_3]$), 1.22–1.28 (m, 4H, $[O-CH_2-CH_2-CH_2-CH_3]$), 1.51–1.31 (ds, 6H, $[CH_3-C-CH_3]$), 3.88 (q, 2H, $[O-CH_2-CH_2-CH_2-CH_3]$), 4.21 (q, 1H, $[C-H_3]$), 4.36 (d, 2H, $[C-H_2]$), 4.57 (q, 1H, $[C-H_2]$), 4.72 (q, 1H, $[C-H_4]$), 5.91 (d, 1H, $[C-H_1]$), 7.10–7.29 (m, 15H, [trityl]).

3-O-Ethyl-1,2-isopropylidene- α -xylopyranoside (13), 3-O-Propyl-1,2-isopropylidene- α -xylopyranoside (14), and 3-O-Butyl-1,2-isopropylidene- α -xylopyranoside (15). These compounds were synthesized by de-O-tritylization¹⁹ of **10**, **11**, and **12**, respectively. Analytical data: **13**, yield = 21.3%. ESMS $[MW + (Na^+)]$: *m/e* 241.16, calcd *m/e* 241.12. 1H NMR ($CDCl_3$) δ , ppm, 1.05 (t, 3H, $[O-CH_2-CH_3]$), 1.51–1.31 (ds, 6H, $[CH_3-C-CH_3]$), 3.28 (t, 2H, $[O-CH_2-CH_3]$), 3.64 (d, 2H, $[C-H_2]$), 4.21 (q, 1H, $[C-H_3]$), 4.47 (q, 1H, $[C-H_2]$), 4.62 (q, 1H, $[C-H_4]$), 5.91 (d, 1H, $[C-H_1]$). **14**, yield = 74.2%. ESMS $[MW + (Na^+)]$: *m/e* 254.96, calcd *m/e* 255.13. 1H NMR ($CDCl_3$) δ , ppm, 1.05 (t, 3H, $[O-CH_2-CH_2-CH_3]$), 1.27 (m, 2H, $[O-CH_2-CH_2-CH_3]$), 1.51–1.31 (ds, 6H, $[CH_3-C-CH_3]$), 3.28 (t, 2H, $[O-CH_2-CH_2-CH_3]$), 3.64 (d, 2H, $[C-H_2]$), 4.21 (q, 1H, $[C-H_3]$), 4.47 (q, 1H, $[C-H_2]$), 4.62 (q, 1H, $[C-H_4]$), 5.91 (d, 1H, $[C-H_1]$). **15**, yield = 34.6%. ESMS $[MW + (Na^+)]$: *m/e* 268.87, calcd *m/e* 269.15. 1H NMR ($CDCl_3$) δ , ppm, 1.05 (t, 3H, $[O-CH_2-CH_2-CH_2-CH_3]$), 1.23–1.28 (m, 4H, $[O-CH_2-CH_2-CH_2-CH_3]$), 1.51–1.31 (ds, 6H, $[CH_3-C-CH_3]$), 3.28 (t, 2H, $[O-CH_2-CH_2-CH_3]$), 3.64 (d, 2H, $[C-H_2]$), 4.21 (q, 1H, $[C-H_3]$), 4.47 (q, 1H, $[C-H_2]$), 4.62 (q, 1H, $[C-H_4]$), 5.91 (d, 1H, $[C-H_1]$).

3-O-Ethyl- α,β -xylopyranose (16), 3-O-Propyl- α,β -xylopyranose (17), and 3-O-Butyl- α,β -xylopyranose (18). These compounds were synthesized from **13**, **14**, and **15**, respectively, as described for **6** using ethyl iodide, propyl iodide, and butyl iodide, respectively. The syrups that were obtained were purified by preparative HPLC, wavelength 220 nm. Analytical data: **16**, yield = 23%; mp 80–84 °C. Anal. Calcd for $C_7H_{14}O_5$: C, 47.18; H, 7.92. Found: C, 46.99; H, 7.77. 1H NMR (D_2O) δ , ppm, 1.04 (t, 3H, $[O-CH_2-CH_3]$), 3.25 (d, 2H, $[C-eH_5]$), 3.29 (t, 2H, $[O-CH_2-CH_3]$), 3.41 (q, 1H, $[C-H_3]$), 3.56 (d, 2H, $[C-aH_5]$), 3.71 (m, 1H, $[C-H_4]$), 3.81 (m, 1H, $[C-H_2]$), (α) 5.71, (β) 4.65 (d, 1H, $[C-H_1]$). ^{13}C NMR (D_2O) δ , ppm, 14.84 ($CH_2CH_2CH_3$), 61.17 (C^5), 63.99 ($CH_2CH_2CH_3$), 68.85 (C^4), 71.04 (C^3), 73.72 (C^2), 92.07 (H α C), 98.15 (H β C). **17**, yield = 29%; mp 78–82 °C. Anal. Calcd for $C_8H_{16}O_5$: C, 49.19; H, 8.72. Found: C, 49.31; H, 8.31. 1H NMR (D_2O) δ , ppm, 1.04 (t, 3H, $[O-CH_2-CH_3]$), 1.39 (m, 2H, $[O-CH_2-CH_2-CH_3]$), 3.25 (d, 2H, $[C-eH_5]$), 3.29 (t, 2H, $[O-CH_2-CH_2-CH_3]$), 3.41 (q, 1H, $[C-H_3]$), 3.56 (d, 2H, $[C-aH_5]$), 3.71 (m, 1H, $[C-H_4]$), 3.81 (m, 1H, $[C-H_2]$), (α) 5.71, (β) 4.65 (d, 1H, $[C-H_1]$). ^{13}C NMR (D_2O) δ , ppm, 14.84 ($CH_2CH_2CH_2CH_3$), 61.17 (C^5), 63.99 ($CH_2CH_2CH_2CH_3$), 64.12 ($CH_2CH_2CH_2CH_3$), 68.85 (C^4), 71.04 (C^3), 73.72 (C^2), 92.07 (H α C), 98.15 (H β C). **18**, yield = 31.0%. Anal. Calcd for $C_9H_{18}O_5$: C, 51.02; H, 7.92. Found: C, 52.11; H, 8.20. 1H NMR (D_2O) δ , ppm, 1.04 (t, 3H, $[O-CH_2-CH_2-CH_2-CH_3]$), 1.24–1.39 (m, 4H, $[O-CH_2-CH_2-CH_2-CH_3]$), 3.25 (d, 2H, $[C-eH_5]$), 3.29 (t, 2H, $[O-CH_2-CH_2-CH_2-CH_3]$), 3.41 (q, 1H, $[C-H_3]$), 3.56 (d, 2H, $[C-aH_5]$), 3.71 (m, 1H, $[C-H_4]$), 3.81 (m, 1H, $[C-H_2]$), (α) 5.67, (β) 4.43 (d, 1H, $[C-H_1]$). ^{13}C NMR (D_2O) δ , ppm, 14.84 ($CH_2CH_2CH_2CH_2CH_3$), 61.17 (C^5), 63.99 ($CH_2CH_2CH_2CH_2CH_3$), 64.12 ($O-CH_2CH_2CH_2CH_2CH_3$), 67.80 ($O-CH_2CH_2CH_2CH_2CH_3$), 68.85 (C^4), 71.04 (C^3), 73.72 (C^2), 92.07 (H α C), 98.15 (H β C).

3-O-Methyl-D-xylose Diethyl Dithioacetal (22). Cold ethanethiol (15 mL) was added to an ice-cold solution of 17.4 g of **3** in 15 mL of 6 M hydrochloric acid. The reaction was left stirring for 12 h and then treated with 2 M sodium carbonate. When the pH became alkaline, 100 mL of acetone and 2.0 g of active carbon

were added to the reaction, and the mixture was filtered. The filtrate was washed with acetone, and the remaining ethanethiol, water, and acetone were distilled out. A syrup was obtained and purified by column silica gel chromatography (ethyl acetate:petroleum ether 30:70). Yield = 76%. ESMS [MW + (Na⁺): *m/e* 293.11, calcd *m/e* 293.10. ¹H NMR (CDCl₃) δ, ppm, 1.93 (t, 6H, [S-CH₂-CH₃]), 2.67 (m, 4H [S-CH₂-CH₃]), 3.56 (s, 3H [O-CH₃]) 3.72 (q, 1H, [C-H3]), 3.77 (m, 2H, [C-H5]), 3.95 (d, 1H, [C-H1]), 4.03 (m, 1H, [C-H4]) 4.08 (q, 1H, [C-H2]).

3-O-Ethyl-D-xylose Diethyl Dithioacetal (23). This compound was synthesized as **22** but using **16** as starting material. Yield = 39.8%. ESMS [MW + (Na⁺): *m/e* 307.78, calcd *m/e* 307.11. ¹H NMR (CDCl₃) δ, ppm, 0.96 (t, 3H, [O-CH₂-CH₃]), 1.93 (t, 6H, [S-CH₂-CH₃]), 2.67 (m, 4H [S-CH₂-CH₃]), 3.53 (q, 2H [O-CH₂-CH₃]), 3.72 (q, 1H, [C-H3]), 3.77 (m, 2H, [C-H5]), 3.95 (d, 1H, [C-H1]), 4.03 (m, 1H, [C-H4]), 4.08 (q, 1H, [C-H2]).

2,4-Benzylidene-3-O-methyl-D-xylose Diethyl Dithioacetal (24). Compound **22** (1.05 g) was dried by three washes with toluene and evaporation. It was then dissolved in 10 mL of dry DMF to which 1.4 mL of benzaldehyde dimethyl acetal, 0.5 g of molecular sieve 3 Å, and 100 mL of dry hydrochloric acid 4 M (in dioxane) were added. The reaction mix was left stirring for 12 h followed by neutralization with 15% (w/v) sodium bicarbonate. The mixture was then filtered, and the filtrate was washed with chloroform and evaporated. Yellow syrup that was obtained was further purified by HPLC using a stepwise gradient of ethyl acetate (10–50%) in petroleum ether. The compound was crystallized from diethyl ether, and 0.29 g of white crystals was obtained. Yield = 11.4%; mp = 47–54 °C. Anal. Calcd for C₁₇H₂₆O₄S₂: C, 56.95; H, 7.31; S, 17.89. Found: C, 56.94; H, 7.18; S, 17.56. ESMS [MW + (K⁺): *m/e* 397.0, calcd *m/e* 397.05. ¹H NMR (CDCl₃) δ, ppm, 1.23 (t, 6H, [S-CH₂-CH₃]), 2.67 (m, 4H [S-CH₂-]), 3.62 (s, 3H [O-CH₃]), 3.72 (q, 1H, [C-H3]), 3.81 (m, 2H, [C-H5]), 3.99 (d, 1H, [C-H1]), 4.23 (m, 1H, [C-H4]), 4.66 (q, 1H, [C-H2]), 5.84 (R), 5.98 (S), *S/R*-ratio 46%/54% (s, 1H, [O-CH-O]), 7.35–7.47 (m, 5H, [Bz]).

2,4-Benzylidene-3-O-ethyl-D-xylose Diethyl Dithioacetal (25). This compound was synthesized as **24** but using **23** as starting material. Yield = 19%; mp = 49–51 °C. Anal. Calcd for C₁₈H₂₈O₄S₂: C, 58.03; H, 7.58; S, 17.21. Found: C, 58.14; H, 7.08; S, 17.36. ESMS [MW + (Na⁺): *m/e* 395.17, calcd *m/e* 395.14. ¹H NMR (CDCl₃) δ, ppm, 0.97 (t, 2H, [O-CH₂-CH₃]), 1.23 (t, 6H, [S-CH₂-CH₃]), 2.67 (m, 4H, [S-CH₂-]), 3.52 (q, 2H, [O-CH₂-CH₃]), 3.72 (q, 1H, [C-H3]), 3.81 (m, 2H, [C-H5]), 3.99 (d, 1H, [C-H1]), 4.23 (m, 1H, [C-H4]), 4.66 (q, 1H, [C-H2]), 5.86 (R), 6.06 (S), *S/R*-ratio 39%/61% (s, 1H, [O-CH-O]), 7.37–7.49 (m, 5H, [Bz]).

Cell Cultures. L6 skeletal myocytes were grown and let to differentiate to multinuclear myotubes (85–95% efficiency) in αMEM supplemented with 2% (v/v) FCS, as described.³⁸ L6 myoblasts expressing c-myc epitope-tagged GLUT1 (GLUT1myc) and GLUT4 (GLUT4myc) were the courtesy of Dr. A. Klip (The Hospital for Sick Children, Toronto, Canada). These cells were grown and let to differentiate into multinucleated myotubes as described.³⁹ A clone of primary cultures of human skeletal muscle myoblasts isolated from *Rectus abdominis* M. of a 38-year-old Caucasian female donor was purchased from PromoCell (clone SkMc-c12530; Heidelberg, Germany). Myoblast cultures were prepared and let to differentiate into multinuclear myotubes using the manufacturer's protocols, media, and reagents.

Hexose Uptake Assay. The rate of [³H]dGlc uptake in myotubes in the absence or presence of insulin was measured as described.⁴⁰ Briefly, L6 myotube cultures were usually preincubated in αMEM supplemented with 2% (v/v) FCS and 23.0 mM D-glucose for 24 h, after which they were treated as described. Insulin effect was measured following its addition (200 nM) to cultures during the last 30 min of treatment. The cultures were then rinsed three times with PBS at room temperature and incubated with PBS, pH 7.4, containing 0.1 mM dGlc and 1.3 μCi/mL [³H]dGlc for 5 min at room temperature. The uptake was stopped by three rapid washes with ice-cold PBS. The PBS solution for the D-xylose uptake assay contained 0.1 mM D-xylose and 1.3 μCi/mL [¹⁴C]xylose. The rate of [³H]-3-O-methyl-D-glucose transport was determined according

to Konrad et al.⁴¹ Briefly, PBS-washed myotubes were incubated with PBS supplemented with 10 μM 3-O-methyl-D-glucose and 5.0 μCi/mL [³H]-3-O-methyl-D-glucose and 0.5 μCi/mL [¹⁴C]sucrose for 90 s at room temperature. The reaction was stopped by three washes with ice-cold PBS containing 20 mM D-glucose, 10 μM cytochalasin B, and 2 mM HgCl₂. Following all uptake assays, the myotubes were then lysed with 0.1% (w/v) SDS in water and taken for liquid scintillation counting of ³H and/or ¹⁴C. The counts of extracellular [³H]-3-O-methyl-D-glucose were calculated from the counts of the extracellular marker [¹⁴C]sucrose and deducted from the total counts of tritium.

MTT Cell Viability Assay. This assay measures the reduction of a tetrazolium component in MTT [3-(4,5-dimethylthiazol-2-yl)-2,5-diphenyl tetrasodium bromide] into an insoluble formazan product by the mitochondria of viable cells.⁴² Myotubes were incubated with MTT (2 mg/mL in αMEM) for 30 min at 37 °C. The medium was then aspirated, DMSO was added to solubilize the colored crystals, and absorbance at 570 nm was measured in an ELISA reader. The amount of color produced is directly proportional to the number of viable cells.

Colorimetric Determination of Surface GLUT1myc and GLUT4myc in L6 Myotubes. Colorimetric detection of surface GLUT4myc or GLUT1myc was performed on the respective myc-tagged L6 myotube cultures as previously described.³⁹ Briefly, cultured myotubes were incubated with rabbit anti-C-Myc antibody (1:200 dilution), washed and fixed with 3% formaldehyde, and further interacted with goat HRP-conjugated anti-rabbit IgG (1:2000 dilution). Following washes, a solution of OPD was added, and the culture plates were taken for absorbance measurement at 492 nM to estimate the relative abundance of GLUT1myc or GLUT4myc on the plasma membrane of myotubes.

Preparation of Cell Lysates and Western Blot Analyses. Whole myotube lysates were prepared as previously described.⁴³ The lysis buffer was 50 mM Tris-HCl, pH 7.5, 1 mM EDTA, 1 mM EGTA, 1 mM Na₃VO₄, 150 mM NaCl, 50 mM NaF, 10 sodium β-glycerophosphate, 5 mM sodium pyrophosphate, and 1 mM PMSF, supplemented with 0.1% (v/v) NP-40, 0.1% (v/v) 2-β-mercaptoethanol, and protease inhibitor cocktail (1:100 dilution). Protein content in the supernatant was determined according to the method of Bradford,⁴⁴ using BSA standard dissolved in the same buffer. Aliquots (5–60 μg of protein) were mixed with sample buffer [62.5 mM Tris-HCl, pH 6.8, 2% (w/v) SDS, 10% (v/v) glycerol, 50 mM DTT, and 0.01% (w/v) bromophenol blue], heated at 95 °C for 5 min, except for samples used for GLUT determinations that were diluted in a urea denaturation buffer [10 mM Tris-HCl, pH 6.8, 8 M urea, 2% (w/v) SDS, 10 mM, and 0.01% (w/v) bromophenol blue], and warmed at 37 °C for 15 min. Proteins were separated on 6–12% SDS-PAGE, and Western blot analyses were performed using antibodies according to the antibody supplier's or previous established protocols. Supporting Information Table 3 gives the main technical details of all buffers used, washing procedures, and antibody dilutions. Following the transfer of proteins from the gel to nitrocellulose membranes and incubation with the second antibody (horseradish peroxidase-conjugated anti-rabbit IgG), the membranes were washed and taken for chemoluminescence detection using the EZ-ECL kit, according to the manufacturer's protocol. Band density measurement was performed after scanning of films using Scion Image software.

ATP Determination. ATP content in lysates of L6 myotubes was measured with the ENLITEN assay kit (Promega, Madison WI). Myotubes in six-well plates were washed three times with cold 0.15 M Tris-HCl, pH 7.75. The wells were then treated with 200 μL of 0.5% (w/v) ice-cold TCA, followed by the addition of 400 μL of this Tris-HCl buffer. The mixture was centrifuged in Eppendorf tubes (12000 rpm, 30 min at 4 °C), and the supernatant fractions were taken for ATP determination according to the manufacturer's instruction. Briefly, aliquots were mixed with recombinant luciferase and D-luciferin. In the presence of oxygen and ATP the enzyme catalyzes the oxidation of D-luciferase to oxyluciferin coupled to hydrolysis of ATP to ADP and pyrophosphate and light emission at 560 nm. The assay was performed in

low-background 96-multiwell plates for fluorescence measurement (Nunc, Roskilde, Denmark) in a Mithras LB-940 luminometer (Berthold Technologies, Bad Willbad, Germany) at room temperature. The ATP standard curve was constructed according to the manufacturer's protocol, using ATP supplied in the kit.

Determination of Protein Binding of 19. Culture medium containing 10% (v/v) FCS was spiked with 4.6–23.0 μM **19** and incubated at 37 °C for 60 min to determine C_i (bound and unbound concentrations). Aliquots were centrifuged in 10 kDa cutoff Microcon tubes (4400g for 60 min; Millipore, Bedford, MA). The protein-free filtrates were collected and analyzed by LC-MS to determine the concentration of free (C_f) **19** in the samples. The protein binding capacity (B) of **19** was calculated by the equation $B (\%) = [(C_i - C_f)/C_i] \times 100$.

The sample for mass spectrometric detection was prepared as follows: Acetonitrile (150 μL) was mixed with 150 μL of filtrates. Testosterone (0.1 μg), which served as an internal standard, was also added. After extraction with 3 mL of *n*-hexane for 1 min and centrifugation (1000g for 7 min) the upper organic layer was separated and evaporated to dryness. The residue was dissolved in 100 μL of acetonitrile, and 20 μL was injected into the LC-MS system. The quantity of **19** was measured using the following system: HPLC-MS Waters Millennium instrument equipped with Waters Micromass ZQ detector, 600 Controller gradient pump, and 717 autosampler (Waters Co., Milford, MA). Settings: nitrogen flow, 500 L/h; source temperature, 400 °C; cone voltage, 35 V; column, XTerra RP-18 (3.5 μm), 2.1 \times 100 mm, heated to 35 °C. The mobile phase (0.3 mL/min) was water and acetonitrile (1:1) containing 0.1% (v/v) formic acid. **19** was monitored at SIR m/z 432 and retained for 24 min. Testosterone was monitored at SIR m/z 289 and retained for 3 min.

Statistical Analysis. Statistical significance ($p < 0.05$) was calculated among experimental groups using the Mann–Whitney test. Results are given as mean \pm SEM ($n = 3$).

Acknowledgment. We are thankful to Mrs. R. Oron and Ms. E. Oliver for excellent technical assistance. S.S., A.H., and Y.K. are members of the David R. Bloom Center for Pharmacy at the Hebrew University of Jerusalem. A.G., D.S., M.B.Y., E.A., and G.C. received fellowships from the Diabetes Research Center of The Hebrew University. This study was supported by grants from the Applied Research Program A of The Hebrew University, The Deutch Foundation for Applied Sciences, Alex Grass Center for Drug Design and Synthesis of Novel Therapeutics, David R. Bloom Center for Pharmacy at The Hebrew University School of Pharmacy, the Nophar Program of the Israel Ministry of Commerce and Trade, and the Israel Science Foundation of The Israel Academy of Sciences and Humanities.

Supporting Information Available: Experimental details of the purity of compounds, data of in vitro assay, chemistry, biological effects, and cytotoxicity of nonactive derivatives, technical details of Western blot analyses, and tracing profiles of lead compounds. This material is available free of charge via the Internet at <http://pubs.acs.org>.

References

- Lann, D.; LeRoith, D. Insulin resistance as the underlying cause for the metabolic syndrome. *Med. Clin. North Am.* **2007**, *91*, 1063–1077.
- Alpert, E.; Totary, H.; Sasson, S. Cellular mediators of glucose-induced autoregulation of hexose transport. In *Frontiers in animal diabetes research: Muscel metabolism*, Zierath, J. R., Walberg-Henriksson, H., Eds.; Taylor & Francis Books, London, 2002; pp 155–167.
- Zierath, J. R.; Kawano, Y. The effect of hyperglycaemia on glucose disposal and insulin signal transduction in skeletal muscle. *Best Pract. Res., Clin. Endocrinol. Metab.* **2003**, *17*, 385–398.
- Ben Yakir, M.; Gruzman, A.; Alpert, E.; Sasson, S. Glucose transport regulators. *Curr. Med. Chem.: Immunol., Endocr. Metab. Agents* **2005**, *5*, 519–527.
- Misra, P. AMP activated protein kinase: a next generation target for total metabolic control. *Expert Opin. Ther. Targets* **2008**, *12*, 91–100.
- Koivisto, U. M.; Martinez-Valdez, H.; Bilan, P. J.; Burdett, E.; Ramlal, T.; Klip, A. Differential regulation of the GLUT-1 and GLUT-4 glucose transport systems by glucose and insulin in L6 muscle cells in culture. *J. Biol. Chem.* **1991**, *266*, 2615–2621.
- Sasson, S.; Cerasi, E. Substrate regulation of the glucose transport system in rat skeletal muscle. Characterization and kinetic analysis in isolated soleus muscle and skeletal muscle cells in culture. *J. Biol. Chem.* **1986**, *261*, 16827–16833.
- Campbell, P. N. Metabolic studies with 3-methyl glucose. II. In vitro studies. *Biochem. J.* **1952**, *52*, 444–447.
- Li, D.; Randhawa, V. K.; Patel, N.; Hayashi, M.; Klip, A. Hyperosmolarity reduces GLUT4 endocytosis and increases its exocytosis from a VAMP2-independent pool in l6 muscle cells. *J. Biol. Chem.* **2001**, *276*, 22883–22891.
- Sasson, S.; Kaiser, N.; Dan-Goor, M.; Oron, R.; Koren, S.; Wertheimer, E.; Unluhizarci, K.; Cerasi, E. Substrate autoregulation of glucose transport: Hexose 6-phosphate mediates the cellular distribution of glucose transporters. *Diabetologia* **1997**, *40*, 30–39.
- Kiyosawa, K. Volumetric properties of polyols (ethylene glycol, glycerol, meso-erythritol, xylitol and mannitol) in relation to their membrane permeability: group additivity and estimation of the maximum radius of their molecules. *Biochim. Biophys. Acta* **1991**, *1064*, 251–255.
- Huguenin, P.; Cochet, B.; Balant, L.; Loizeau, E. D-Xylose absorption test. A pharmacokinetic and statistical study. *Schweiz. Med. Wochenschr.* **1978**, *108*, 206–214.
- Bollenback, G. Methyl-alpha-D-glucopyranoside. In *Methods in Carbohydrate Chemistry*; Whistler, R., Wilfrom, M., BeMiller, J., Eds.; Academic Press: New York, 1963; Vol. 2, pp 326–327.
- Moravcova, J.; Capkova, J.; Stanek, J. One-pot synthesis of 1,2-O-isopropylidene-alpha-D-xylopyranose. *Carbohydr. Res.* **1994**, *263*, 61–66.
- Bowering, W. An alternative synthesis of 2-O-methyl-D-xylose. *Can. J. Chem.* **1958**, *36*, 283–284.
- Levine, P.; Raymond, A. 3-Methyl-xylose and 5-methyl-xylose. *J. Biol. Chem.* **1933**, *102*, 317–324.
- Takeo, K.; Murata, Y.; Kitamura, S. A facile synthesis of 4-O-allyl-D-xylopyranoses and it's in the preparation of xylo-oligosaccharides. *Carbohydr. Res.* **1992**, *224*, 311–318.
- de Bruyne, C. K.; Loontjens, F. G. Synthesis of alkyl beta-xylopyranoside in the presence of mercuric salts. *Nature* **1966**, *209*, 396–397.
- Ly, Y.; Just, G. Study on the diastereoselective synthesis of dithymidine phosphorothionates through a D-xylose derived chiral auxiliary and development of novel catalyst. *Tetrahedron Lett.* **2000**, *41*, 9223–9227.
- Silverman, R. B. *The organic chemistry of drug design and drug action*; Academic Press: San Diego, 1992; pp 352–396.
- Silverman, R. B. *The organic chemistry of drug design and drug action*; Academic Press: San Diego, 1992; pp 289–319.
- Nomura, M.; Shuto, S.; Matsuda, A. Synthesis of the cyclic and acyclic acetal derivatives of 1-(3-C-ethynyl-beta-D-ribo-pentofuranosyl)cytosine, a potent antitumor nucleoside. Design of prodrugs to be selectively activated in tumor tissues via the bio-reduction-hydrolysis mechanism. *Bioorg. Med. Chem.* **2003**, *11*, 2453–2461.
- Curtis, J.; Jones, K. The synthesis of 3-O-beta-D-xylopyranosyl-D-xylose. *Can. J. Chem.* **1960**, *38*, 1305–1315.
- Ferrier, R.; Hatton, L. The acid-catalyzed condensation of D-xylose with benzaldehyde in the presence of alcohols. Two diastereoisomeric 1,2:3,5-di-O-benzylidene-alpha-D-xylofuranoses. *Carbohydr. Res.* **1967**, *5*, 132–139.
- Rao, S. P.; Grindley, T. B. The reduction of benzylidene derivatives of pentose diethyl dithioacetals with lithium aluminium hydride-aluminium trichloride. *Carbohydr. Res.* **1991**, *218*, 83–93.
- Eros, D.; Kovcsdi, I.; Orfi, L.; Takacs-Novak, K.; Acsady, G.; Keri, G. Reliability of log P predictions based on calculated molecular descriptors: A critical review. *Curr. Med. Chem.* **2002**, *9*, 1819–1829.
- Zaid, H.; Antonescu, C. N.; Randhawa, V. K.; Klip, A. Insulin action on glucose transporters through molecular switches, tracks and tethers. *Biochem. J.* **2008**, *413*, 201–215.
- Khan, A. H.; Pessin, J. E. Insulin regulation of glucose uptake: a complex interplay of intracellular signalling pathways. *Diabetologia* **2002**, *45*, 1475–1483.
- Kanai, F.; Ito, K.; Todaka, M.; Hayashi, H.; Kamohara, S.; Ishii, K.; Okada, T.; Hazeki, O.; Ui, M.; Ebina, Y. Insulin-stimulated GLUT4 translocation is relevant to the phosphorylation of IRS-1 and the activity of PI3-kinase. *Biochem. Biophys. Res. Commun.* **1993**, *195*, 762–768.
- Barnett, S. F.; Defeo-Jones, D.; Fu, S.; Hancock, P. J.; Haskell, K. M.; Jones, R. E.; Kahana, J. A.; Kral, A. M.; Leander, K.; Lee, L. L.; Malinowski, J.; McAvoy, E. M.; Nahas, D. D.; Robinson, R. G.; Huber, H. E. Identification and characterization of pleckstrin-homology-

- domain-dependent and isoenzyme-specific Akt inhibitors. *Biochem. J.* **2005**, *385*, 399–408.
- (31) Bouzakri, K.; Zachrisson, A.; Al-Khalili, L.; Zhang, B. B.; Koistinen, H. A.; Krook, A.; Zierath, J. R. siRNA-based gene silencing reveals specialized roles of IRS-1/Akt2 and IRS-2/Akt1 in glucose and lipid metabolism in human skeletal muscle. *Cell Metab.* **2006**, *4*, 89–96.
- (32) Kramer, H. F.; Witezak, C. A.; Fujii, N.; Jessen, N.; Taylor, E. B.; Arnolds, D. E.; Sakamoto, K.; Hirshman, M. F.; Goodyear, L. J. Distinct signals regulate AS160 phosphorylation in response to insulin, AICAR, and contraction in mouse skeletal muscle. *Diabetes* **2006**, *55*, 2067–2076.
- (33) Fujii, N.; Hirshman, M. F.; Kane, E. M.; Ho, R. C.; Peter, L. E.; Seifert, M. M.; Goodyear, L. J. AMP-activated protein kinase alpha2 activity is not essential for contraction- and hyperosmolarity-induced glucose transport in skeletal muscle. *J. Biol. Chem.* **2005**, *280*, 39033–39041.
- (34) Isakovic, A.; Harhaji, L.; Stevanovic, D.; Markovic, Z.; Sumarac-Dumanovic, M.; Starcevic, V.; Micic, D.; Trajkovic, V. Dual anti-glioma action of metformin: cell cycle arrest and mitochondria-dependent apoptosis. *Cell. Mol. Life Sci.* **2007**, *64*, 1290–1302.
- (35) Bruss, M. D.; Arias, E. B.; Lienhard, G. E.; Cartee, G. D. Increased phosphorylation of Akt substrate of 160 kDa (AS160) in rat skeletal muscle in response to insulin or contractile activity. *Diabetes* **2005**, *54*, 41–50.
- (36) Hawley, S. A.; Gadalla, A. E.; Olsen, G. S.; Hardie, D. G. The antidiabetic drug metformin activates the AMP-activated protein kinase cascade via an adenine nucleotide-independent mechanism. *Diabetes* **2002**, *51*, 2420–2425.
- (37) Musi, N.; Hirshman, M. F.; Nygren, J.; Svanfeldt, M.; Bavenholm, P.; Rooyackers, O.; Zhou, G.; Williamson, J. M.; Ljunqvist, O.; Efendic, S.; Moller, D. E.; Thorell, A.; Goodyear, L. J. Metformin increases AMP-activated protein kinase activity in skeletal muscle of subjects with type 2 diabetes. *Diabetes* **2002**, *51*, 2074–2081.
- (38) Bashan, N.; Burdett, E.; Guma, A.; Sargeant, R.; Tumiati, L.; Liu, Z.; Klip, A. Mechanisms of adaptation of glucose transporters to changes in the oxidative chain of muscle and fat cells. *Am. J. Physiol.* **1993**, *264*, C430–C440.
- (39) Wang, Q.; Khayat, Z.; Kishi, K.; Ebina, Y.; Klip, A. GLUT4 translocation by insulin in intact muscle cells: Detection by a fast and quantitative assay. *FEBS Lett.* **1998**, *427*, 193–197.
- (40) Alpert, E.; Gruzman, A.; Studler-Lardi, B.; Blejter, R.; Reich, R.; Sasson, S. COX-2 inhibitors augment the rate of hexose transport in L6 skeletal myotubes. *Diabetologia* **2006**, *49*, 562–570.
- (41) Konrad, D.; Rudich, A.; Bilan, P. J.; Patel, N.; Richardson, C.; Witters, L. A.; Klip, A. Troglitazone causes acute mitochondrial membrane depolarisation and an AMPK-mediated increase in glucose phosphorylation in muscle cells. *Diabetologia* **2005**, *48*, 954–966.
- (42) Mutoh, T.; Kumano, T.; Nakagawa, H.; Kuriyama, M. Involvement of tyrosine phosphorylation in HMG-CoA reductase inhibitor-induced cell death in L6 myoblasts. *FEBS Lett.* **1999**, *444*, 85–89.
- (43) Alpert, E.; Gruzman, A.; Totary, H.; Kaiser, N.; Reich, R.; Sasson, S. A natural protective mechanism against hyperglycaemia in vascular endothelial and smooth-muscle cells: Role of glucose and 12-hydroxyicosatetraenoic acid. *Biochem. J.* **2002**, *362*, 413–422.
- (44) Bradford, M. M. A rapid and a sensitive method for the quantitation of microgram quantities of protein utilizing the principle of protein-dye binding. *Anal. Biochem.* **1972**, *72*, 248–254.

JM8008713